Photoinduced electron transfer in triazole-bridged donor-acceptor dyads - A critical perspective

Caroline Müller, Sébastian Bold, Murielle Chavarot-kerlidou, Benjamin Dietzek-Ivanšić

Coordination Chemistry Reviews 472 (2022) 214764

Contents lists available at ScienceDirect

Coordination Chemistry Reviews

journal homepage: www.elsevier.com/locate/ccr

Review

Photoinduced electron transfer in triazole-bridged donor-acceptor dyads – A critical perspective

Carolin Müller [a,b,1], Sebastian Bold [a,b,c,1], Murielle Chavarot-Kerlidou [c], Benjamin Dietzek-Ivanšić [a,b,d,*]

[a] Institute of Physical Chemistry, Friedrich Schiller University Jena, Helmholtzweg 4, Jena 07743, Germany
[b] Department Functional Interfaces, Leibniz Institute of Photonic Technology Jena (Leibniz-IPHT), Albert-Einstein-Straße 9, Jena 07745, Germany
[c] Université Grenoble Alpes, CNRS, CEA, IRIG, Laboratoire de Chimie et Biologie des Métaux, 17 rue des Martyrs, Grenoble F-38000, France
[d] Center for Energy and Environmental Chemistry Jena (CEEC Jena), Friedrich Schiller University Jena, Philosophenweg 8, Jena 07743, Germany

ARTICLE INFO

Article history:
Received 26 April 2022
Accepted 3 August 2022
Available online 24 August 2022

Keywords:
CLICK chemistry
Electron transfer
Triazole linker
Donor-acceptor dyads
Photocatalysis

ABSTRACT

In recent years, dyads in which molecular donor and acceptor moieties are chemically linked by a bridging ligand have emerged as attractive systems for light-driven catalysis. Their modular structure, controllable donor-acceptor distance, and their ability to undergo light-driven charge transfer, which is not limited by diffusion, render such systems promising in light-driven charge-transfer reactions and light-driven redox catalysis. Copper-catalyzed alkyne azide cycloaddition (CuAAC) is a particularly popular synthetic strategy for coupling donor and acceptor moieties. This CLICK chemistry approach yields dyads with a 1,2,3-triazole bridging motif. In this review, we discuss the complex role played by this triazole linker to drive electron transfer (eT) in a respective triazole-bridged donor-acceptor dyad upon photoexcitation. We review how structural and electronic properties of the bridge influence charge separation and recombination rates. Furthermore, the role of the triazole bridge energetics in thermal as well as oxidative and reductive photoinduced eT will be discussed. Finally, criteria for the design of dyads with different eT properties are derived.

Contents

1. Introduction

Electron transfer (eT) is a key step in biological and chemical processes, *e.g.*, for the conversion and storage of energy [1]. Inspired by photosynthesis, the development of artificial photosynthetic systems has become an increasingly important area of research [2–4]. The catalytic activity in these systems is based on long-lived and long-range charge separated states, which are

Abbreviations: CuAAC, Copper-catalyzed alkyne azide cycloaddition; eT, electron transfer; EnT, energy transfer; CS, charge separation; CR, charge recombination; hT, hole transfer; HOMO, highest-occupied molecular orbital; LUMO, lowest-unoccupied molecular orbital.

* Corresponding author at: Institute of Physical Chemistry and Abbe Center of Photonics, Friedrich Schiller University Jena, Helmholtzweg 4, Jena 07743, Germany.
E-mail address: benjamin.dietzek@uni-jena.de (B. Dietzek-Ivanšić).

[1] These authors contributed equally.

https://doi.org/10.1016/j.ccr.2022.214764
0010-8545/

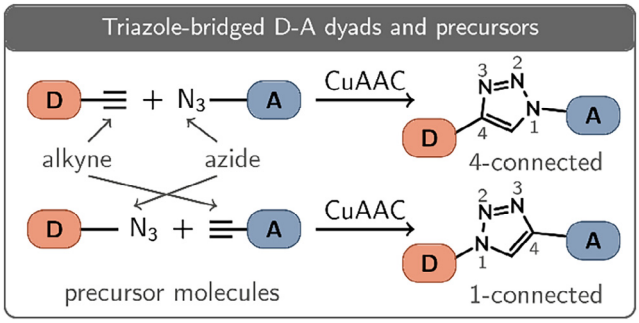

Fig. 1. Schematic structure of 1- and 4-connected triazole-bridged D–A dyads and the corresponding alkyne- and azide-substituted precursors. The building blocks are *clicked* together *via* a copper-catalyzed alkyne-azide cycloaddition (CuAAC) reaction.

generated *via* eT processes initiated by light absorption [5–9]. Fundamental information on such light-induced eT processes has been provided from systems in which a donor (D) and an acceptor (A) molecular units are chemically linked by a molecular bridge [10–17]. The main advantage of D-A dyads compared to the corresponding bimolecular systems is that complex factors arising from diffusion in solution and the inhomogeneous distribution of D-A distances are eliminated. This, on the one hand, enables to obtain important information about the dependencies of the eT processes on, *e.g.*, the D–A distance and the electronic coupling of the D- and A-units in the excited state. On the other hand, the molecular bridge can play a critical role in driving eT between the D- and A-units rather than serving as an inert *spacer*, i.e., a molecular motif that only tunes the D-A distance [18–22].

A very popular synthetic strategy for the coupling of D- and A-units is the copper-catalyzed alkyne-azide cycloaddition (CuAAC, see Fig. 1), forming a 1,4-disubstituted 1,2,3-triazole ring [23–27]. This so-called CLICK-reaction is indeed a highly versatile and high-yielding coupling procedure, compatible with many organic and metal-organic functions, and operating at mild reaction conditions. It can thus provide a straightforward and modular synthetic access to a wide variety of D-A dyads.

Due to their functional diversity, 1,2,3-triazoles are versatile building blocks [28–31] for a wide range of applications, *e.g.*, as ligand in metal complexes [32], H-bond donor/acceptor [33], anion receptor [34], anchoring group on metal surfaces [35], or linker promoting [36–55] or preventing [18,45,46,56–70] intramolecular charge transfer. The conjugated nature of the linker might seem promising to drive eT across that bridge. However, its suitability as a linker in D–A dyads is disputed in literature; literature examples report on systems in which intramolecular eT across the triazole-bridge efficiently takes place within picoseconds [36–55] or nanoseconds [46,49,71–76]. However, also systems are reported in which eT could not be observed at all, despite favorable thermodynamics [18,45,56–70,77].

This review takes a critical perspective and discusses the role played by the triazole bridge in enabling eT between D- and A-units in D–A dyads. A quantitative and mechanistic comparison of different triazole-bridged D–A dyads to draw general conclusions about their photoinduced eT properties is quite difficult due to the large parameter space to be considered when tuning the eT properties. To derive inherent properties of triazole linkers on the eT properties, we first focus on the dependence of the charge separation and recombination rates (k_{CS} and k_{CR}) on structural (***flexibility*** ↔ ***conjugation***) and electronic properties (***conjugation*** ↔ ***connectivity***) of the linker (*Section 2.1*). This includes the D–A distance (d_{DA}), the relative energy of the D-centered highest occupied molecular orbital (HOMO, oxidation potential) with respect to the A-centered lowest unoccupied MO (LUMO, reduction potential), as well as the energy barrier ($\Delta G^{\ddagger}$) and driving force of the eT (ΔG^{0}, see Fig. 3a). In this context, we will differentiate – depending on the relative energy of the bridge orbitals – between through-bond and through-space eT. Subsequently, we discuss the charge separation processes putting emphasis on the mechanistic differences between photoinduced oxidative and reductive processes (*Section 2.2*) as well as between photoinduced and thermal charge-transfer processes (*Section 2.3*). Finally, we will conclude about the impact of the triazole bridge on the photoinduced charge transfer processes based on the individual parameters mentioned above. Selected examples illustrate specific factors of the triazole bridges driving eT in D–A dyads. Overall, this review tries to provide a comprehensive overview of the light-induced eT kinetics in triazole-bridged D-A systems.

2. Modules of triazole-bridged D-A dyads and basic mechanistic considerations

Most of the triazole-bridged D–A dyads, for which charge transfer processes or photoredox properties have been investigated, consist of a light-absorbing D-moiety bound to an A-unit either covalently or by complexation to a metal ion (see Fig. 2). One of the most popular choice of donor units are Zn^{II} porphyrins (*e.g.* **D1a** and **D1b**, *cf.* Fig. 2a) [38,41,46,48–51,57,59–63,65,66,70,73,75, 78–81], followed by poly(fluorene) [40,44,45,52] and poly(thiophene) polymers [42–44], BODIPY (see **D4a** and **D4b** in Fig. 2a) [58,67, 69,74,77,82] and organic push–pull dyes [36,37,54,83,84], as well as Ru^{II} polypyridyl-type complexes (see **D2a–c** in Fig. 2a) [18,67,71,72,76,85–89]. The most common acceptor units in D–A dyads are fullerenes [38,48–51,53,54,59,60,70,73] (see **A1** in Fig. 2b), diimide chromophores (see **A3a** and **A3b** in Fig. 2b) [46,55,72,90–92], Dawson-type (α_2-$P_2W_{17}O_{61}$) polyoxometalates (POMs, see **A2** in Fig. 2b) [75,77,78,93], and metal complexes (*e.g.*, with central Ru^{II} [42–45,52,67,88,94], Fe^{IV} [88], Ni^{II} [87], Cu^{II} [41,68,86], Co^{III} [36,37,64,84,85], Re^{I}- [76], or Rh^{III}-ions [18], *cf.* **A4** and **A5** in Fig. 2b).

In photoactive triazole-bridged D–A dyads (**D–*trz*–A**) intramolecular charge separation (*photoinduced* eT, *cf.* Fig. 3b) can take place after photoexcitation of either the D- or the A-unit, depending on the chemical design of the particular dyad [46,55]. However, if external sacrificial reductants or oxidants are available, intermolecular reductive (or oxidative) quenching of the excited state can compete with the intramolecular photoinduced eT. If the intermolecular quenching process is faster than the intramolecular one, the resulting species containing a reduced (or oxidized) photocenter can undergo a thermally driven intramolecular eT *(thermal eT)*. In other words, the *thermal eT* refers to D-to-A eT which occurs in the electronic ground state after single-electron reduction of the D- (see Fig. 3a) or oxidation of the A-unit.

According to the superexchange model, photoinduced D-to-A eT occurs in a single, coherent step [95] in **D–*trz*–A** systems. In this mechanism, it is assumed that no discrete bridge-centered states are populated, but that bridge-centered orbitals contribute to the electronic coupling of the D and A unit [95–98]. Mostly, a direct coupling between the D- and A-unit of D–B–A dyads in the ground state is negligible [95]. Generally, there are two superexchange mechanisms that describe D-to-A eT:

- Let us first consider *photoinduced eT* processes after photoexcitation of the D-moiety: Electron transfer from the photoexcited D to the A unit is mediated by the bridge-centered unoccupied molecular orbitals (see Fig. 3b, left half). Such states are also key when considering the (ground state) electron transfer from a photoreduced donor to the acceptor unit, i.e., *thermal eT* (**$D^{\bullet-}$–*B*–A** → **D–*B*–$A^{\bullet-}$**, see Fig. 3a).

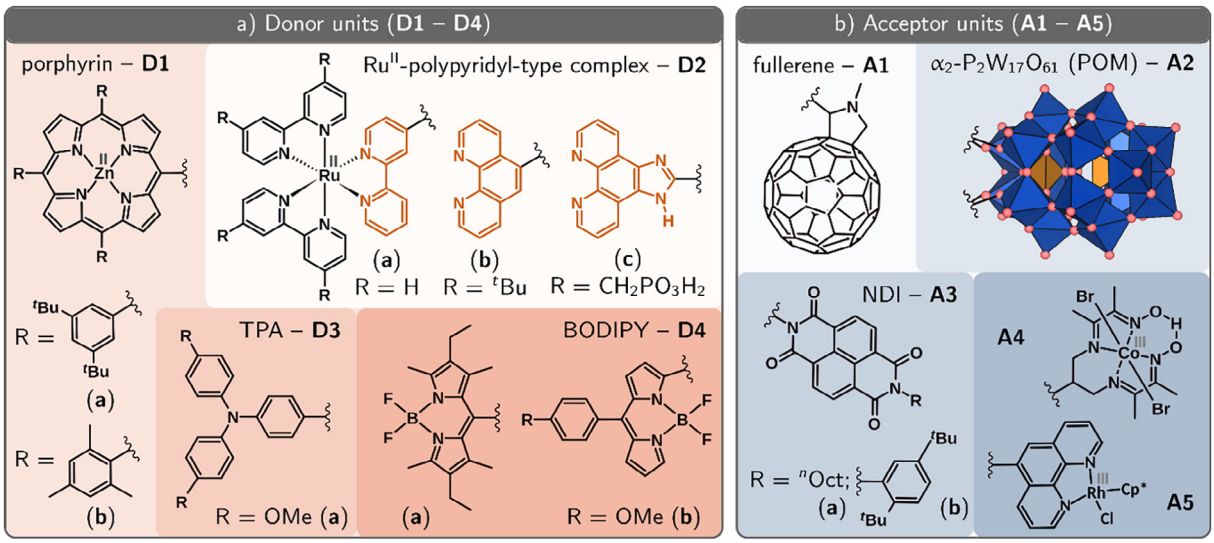

Fig. 2. Structures of donor- (**D1-D4**, a) and acceptor-units (**A1-A5**, b) of selected triazole-bridged D-A dyads employed to study electron transfer (eT) processes (*e.g.*, charge separation and -recombination) across the triazole CLICK-bridges. The respective D- and A-moieties are categorized into metal complexes (**D1**, **D2**, **A4**, and **A5**), organic dyes (**D3**, **D4**, and **A3**), fullerenes (**A1**), and Dawson-type polyoxometalates (**A2**).

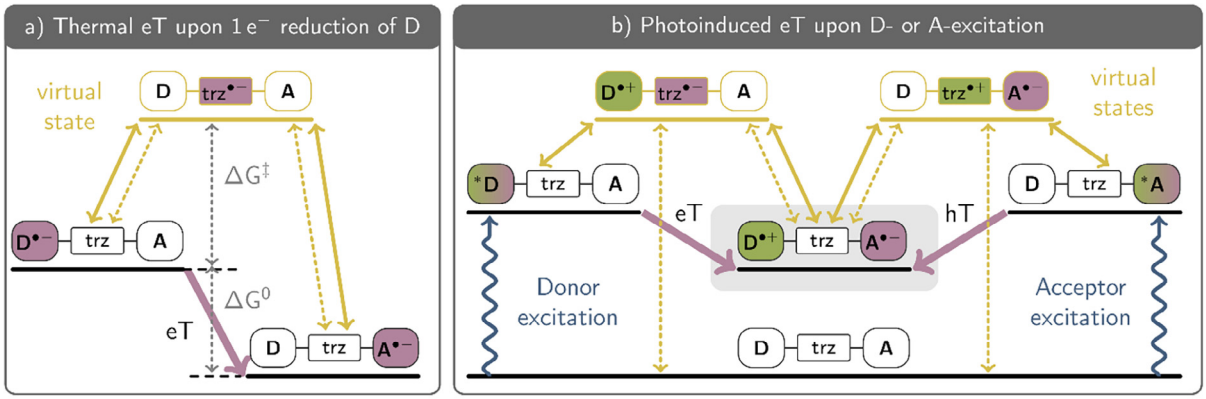

Fig. 3. Schematic representation of thermal and photoinduced intramolecular through-bond eT processes in triazole-bridged D–A dyads mediated by superexchange: a) *Thermal eT* ($D^{\bullet-}$–trz–A → D–trz–$A^{\bullet-}$) occurring after reductive quenching of a D-centered photoexcited state by an external sacrificial electron donor. The D–to–A eT involves a triazole-centered virtual state (D–$trz^{\bullet-}$–A), *i.e.*, it occurs *via* a LUMO-mediated superexchange eT. b) *Photoinduced eT* following excitation of the D- (left, *oxidative photoinduced eT*) or A-moiety (right, *reductive photoinduced eT*). The effective photoinduced charge separation is mediated *via* a *donor-to-bridge eT* ($D^{\bullet+}$–$trz^{\bullet-}$–A) or an *acceptor-to-bridge hT* (D–$trz^{\bullet+}$–$A^{\bullet-}$), respectively. The charge recombination paths are indicated by dashed lines.

- Let us now consider the charge transfer processes after photoexcitation of the A-unit: When A is electronically excited, it can be reductively quenched by intramolecular electron transfer from the donor unit. Such intramolecular eT is generally considered as photoinduced *hole transfer* and involves occupied molecular orbitals centered on the bridge (see Fig. 3b, right half). These orbitals are also essential in mediating thermally-driven electron transfer from the donor unit to the photo-oxidized acceptor (having transferred its electron to a sacrificial oxidant).

Therefore, to design triazole-bridged dyads with predictable eT characteristics, it is important to understand the role of the structure and electronics of the triazole in driving eT.

3. Detailed investigations of charge transfer processes in triazole-bridged D-A dyads

3.1. Through-bond vs. through-space eT

Before entering more detailed considerations about the structural and electronic properties of triazole-bridges that determine the eT properties of their respective D–A dyads [48,51,55,60,75,93,99,100], we consider possible electron transfer mechanisms that can occur in molecular dyads [95]. Generally, not only through-bond eT (intramolecular eT) across the bridge is conceivable. Also through-space eT might be operative in dyads if the D- and A-units can come sufficiently close to each other [48,58,93,101]. The two mechanisms can be discriminated by varying the nature of the solvent. The kinetics of through-bond eT (*cf.* Fig. 3) depends on the solvent polarity, while this is not the case for through-space eT [48]. Without considering specific molecular structures, it is noteworthy that both mechanisms require distinct conditions to be met. Through-space eT quite generally requires a high ***flexibility*** of the molecular linker [48,58,93,101] since it is mediated by intramolecular π–π dipolar interactions between the D- and A-units (orbital overlap). This flexibility allows the molecular dyads to sample a large conformational space (both with respect to the D-A distance and to the mutual D-A orientation). Thereby, the dyad encounters molecular geometries which favor through-space electron transfer [48]. Through-bond eT, on the other hand, is sensitive to the energy levels of the donor, acceptor, and bridging units and requires at least partial electronic coupling

between the donor and the bridge as well as the bridge and the acceptor unit. Therefore, through-bond eT is affected by the ***connectivity*** of the triazole regarding the position of the carbon and nitrogen atoms, which affects the energy levels of the different units [48,55,60], and the ***conjugation*** of the linker [75]. According to Marcus theory, the electron transfer in D–*B*–A systems is essentially governed by the bridge energetics ($\Delta G^{\ddagger}$) and reorganization energy (λ). The latter term is dependent on many factors, such as the conformational dynamics of the bridge and solvents [102]. With respect to solvent dependence, the literature on triazole-bridged dyads [18,48,49,73,74] shows the expected behavior; as with other bridging ligands, electron transfer efficiency increases upon transition from non-polar to polar solvents [102–104]. Therefore, we confine the following discussion to the influence of the bridge conformation on charge transport in D–*B*–A molecules.

Linker flexibility. In the literature, D-A dyads have been synthesized with linkers with very different flexibility, from fully rigid bridges [38,46,48–51,55,57,60–62,64,67,72,75,76,82,86,89,92] to flexible chains [40,42–45,47,51–54,57,63,65,66,69–71,73–75,77,83,88,91,93,101]. Linker flexibility is achieved by elements that allow rotation around bonds of sp^3-hybridized atoms, such as in alkyl chains. However, also mostly conjugated systems with some degree of rotational flexibility can be designed, *e.g.*, resorting to non-*para*-substitution on phenylene-triazole-phenylene linkers (see Fig. 4b) [48,49,51,60,105]. Changing the flexibility of the linker does not *a priori* affect the electronic coupling in the dyads but rather the average D-A distance (d_{DA}). A high degree of flexibility can enable a short D-A distance (d_{DA}), as the dyad can at least partially double back on itself (see structure of **D1a–*m4m*–A1** in Fig. 4c). Contrarily, high rigidity of the linker prevents this, but allows a precise control of the D-A distance (see d_{DA} of **D1a–*p4p*–A1** in Fig. 4a and c).

Controlling d_{DA} can be a design advantage by analogy to photosynthetic systems, where the redox cofactors are embedded at optimal mutual distances, essentially preventing charge recombination [48]. Between the two extremes, linkers are found with just a few elements that afford flexibility such as rotation around bonds of sp^3-hybridized atoms [50,51,58–61,70,74,75,77,80,81,87,88,94,106–108]. For these semi-rigid linkers, the D–A distance is not easily identifiable. Consequently, some ambiguity in the nature of the eT mechanism might arise since depending on the specific orientation of the semi-rigid and semi-conjugated linker, both, through-bond and through-space eT, might contribute to the observed photoinduced eT [87,88].

There are reports in literature of D-A dyads with flexible [40,42–45,51–54,57,63,65,66,69–71,73–75,83,88,91,93,101], semi-rigid [36,41,50,58,68,77–81,84,87,93,94], and rigid triazole bridges [23,38,46,48–51,55,57,60–62,72,75,76,82,86,89,92] showing photoinduced eT. The timescale of charge separation is found to be independent of the linker structure and can range from a few ps [48–54] up to some ns and µs [46,49,71,76,79,82,86–89,91]. For example, dyads with rigid linkers showing eT on sub-ns- [48,49], ns- [46,76,82], and µs- timescale [71,86] are mentioned in literature. Similarly, sub-ns eT processes have also been reported for semi-rigid [50,51] and flexible [52–54] systems. This indicates that sufficiently high electronic couplings can be achieved in any approach linking D- and A-units. Consequently, it can be concluded that each of the underlying design principles has its merits and pitfalls, and none of them is generally ill- or well-suited for implementing intramolecular eT reactions.

Of special interest are those systems that undergo ultrafast intramolecular eT, *i.e.*, that show intramolecular charge separation on a ps-timescale. Such sub-ns processes have been reported for flexible and rigid systems, although the charge transfer mechanisms of the molecules studied in the two categories differ: Systems with flexible linkers that display ultrafast eT include, for instance, polymer-based dyads (τ_{ET} = 0.2 – 2 ps) [40,42–45]. In polymers, mainly through-space eT and energy transfer (EnT) processes occur due to the spatial proximity of the A- and photoexcited D-unit. The frequent through-space eT in polymers stems from the flexibility of the polymer coil and the high number of D- and A-units present on a single polymer chain. Similarly, fast (τ_{ET} < 20 ps) through-space eT has also been observed for flexible and not-conjugated porphyrin-POM dyads [51,75]. Contrary, the charge transfer processes in rigid systems rely on through-bond eT [38,46,49,55,76]. Among the dyads with rigid linkers showing sub-ns charge separation are a TPA-NDI (**D3a–*p4p*–A3b**) [55] and a porphyrin–NDI (**D1b–*p1p*–A3b**) dyad [46]. It is important to note that in these systems, the NDI acceptor unit rather than the donor units were excited, so that charge separation occurs *via* a hole transfer (hT, *cf.* *Section 3.2*).

One concern of using flexible linkers is that charge recombination might be enhanced since the D- and A-units are in proximity in the geometry in which forward eT takes place. As a result, a charge-separated state is formed in which the D- and A-units are in proximity, which in turn can promote a rapid back-electron transfer. This scenario is exemplified in a study by *Campidelli et al.*, who investigated porphyrin-fullerene dyads linked either by a rigid (see geometry of ***p1p*** in Fig. 6c) or a flexible linker (***1p***) containing a central phenyl group connected *via* methylene groups at the *meta*-position that yields the linker flexibility [51]. Both dyads show charge separation on the ps-timescale. However, the studied dyads differ with respect to the eT mechanism: While **D1a–*p1p*–A1** shows through-bond eT, through-space eT occurs in the dyad with the flexible linker (**D1a–*1p*–A1**). Nevertheless, the rigidification of the linker slows down the charge recombination to 650 ns in the rigid (**D1a–*p1p*–A1**) *vs.* 286 ns in the more flexible dyad (**D1a–*1p*–A1**) [51]. Overall, charge recombination in triazole-linked D–A dyads tends to take place faster in systems with flexible linkers [38,40–43,45,46,48–51,54,55,73,79,80,83,84,86,93]. However, this effect is not strongly pronounced; most of the systems with flexible linkers show charge recombination between 6 and 500 ns [45,51,54,73], while most rigid system do so between 400 ns and 2 µs [46,48,49,51,76].

The specific role of linker flexibility was also evaluated by *Harriman et al.*, who studied the eT properties in a series of porphyrin-POM (POM: Dawson-type (α_2-$P_2W_{17}O_{61}$) polyoxometalate) dyads. The authors investigated the rigid and conjugated dyad **D1a–*p4p*–A2** as well as the flexible and non-conjugated dyads **D1a–*p4*–A2** and **D1a–*4*–A2** (see Fig. 5) [75,93]. In **D1a–*p4p*–A2** no oxidative electron transfer to the POM was observed despite a sufficiently large driving force for eT of −1.16 eV [75]. Allowing for a flexible linker (**D1a–*p4*–A2** or **D1a–*4*–A2**) by integrating an alkyl group, enabled eT on a characteristic timescale of 20 – 200 ps [75]. It is concluded that the triazole linker is a poor conductor of electronic charge resulting in slow through-bond eT despite a high thermodynamic driving force. In the rigid dyad (**D1a–*p4p*–A2**) eT occurs primarily *via* bimolecular processes between two dyad molecules, *i.e.*, it relies on diffusion-controlled intermolecular interactions between the porphyrin triplet state as donor and the POM as electron acceptor (τ_{CS} > 2 ns) [75]. In dyads with flexible linkers, D-to-A eT occurs in *circa* 20 ps. This significantly shorter τ_{CS} is caused by the flexible linker, which allows for the spatial proximity between the photoexcited D- and A-units and thus facilitates through-space electron transfer; thereby it circumvents the limitation of through-bond electron transfer (see Fig. 5). However, this causes accelerated eT in both directions, namely, charge separation and -recombination.

Similar observations were made when combining the same α_2-$P_2W_{17}O_{61}$ polyoxometalate acceptor with perylene mono-imides (PMI) as donors into D-A dyads [93]. In these systems, replacement of a semi-rigid linker (phenylene-methylene group) by a shorter,

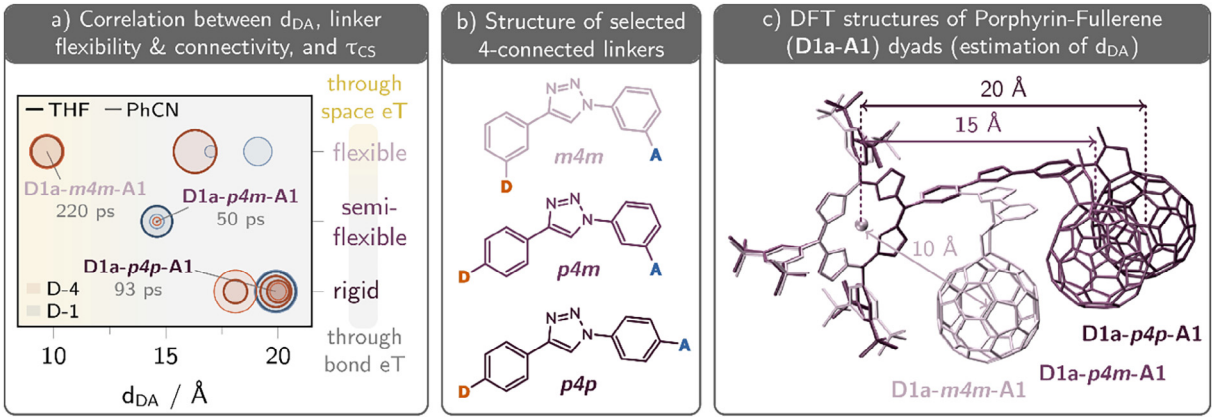

Fig. 4. Summary of electron transfer properties in triazole-bridged porphyrin-fullerene dyads of different flexibility, conjugation and connectivity: a) Correlation between the donor-acceptor distance (abscissa: d_{DA}), linker flexibility (ordinate: classification of the linker into rigid, semi-flexible, or flexible), linker connectivity (orange: 4-connected, blue: 1-connected), and charge separation rate (diameter of the symbols: τ_{CS},) of porphyrin-fullerene (**D1a–A1**) dyads in benzonitrile (PhCN) [38,48,49,73] and tetrahydrofuran (THF) [38,48,50,51]. The respective regions of through-space and through-bond eT are highlighted in gold and grey, respectively. b) Structural formula of selected conjugated, 4-connected linkers of different flexibility (***m*** and ***p*** refer to the *meta* or *para*-substitution on the phenyl rings whereas ***1*** and ***4*** refer to the connectivity on the triazole ring with respect to the D-moiety), *i.e.*, ***p4p*** (rigid), ***p4m*** (semi-flexible), and ***m4m*** (flexible). c) Optimized 3D-structures of **D1a–*p4p*–A1**, **D1–*p4m*–A1**, and **D1a–*m4m*–A1** obtained at the DFT level of theory (C, N, H: *B3LYP/Def2TZVP* [109–111], Zn: *B3LYP/Def2TZVP+LANL2DZ* [109–112]). The respective d_{DA} values correspond to center-to-center distances as indicated by the double-arrows. (For interpretation of the references to colour in this figure legend, the reader is referred to the web version of this article.)

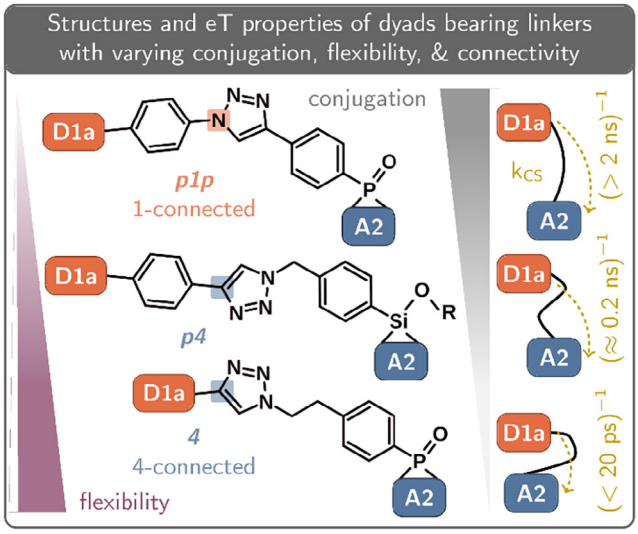

Fig. 5. Structural formulas of the triazole bridges of the porphyrin-POM dyads **D1a–*p1p*–A2**, **D1a–*p4*–A2**, and **D1a–*4*–A2**. While only the rigid **D1a–*p1p*–A2** is fully conjugated, the flexibility of the linker increases following the order ***p1p*** < ***p4*** < ***4*** (see violet bar) [75]. It was found that the charge separation rates (k_{CS}, given in the right column of the figure) upon photoexcitation of the porphyrin-unit (**D1a**) increase with increasing flexibility, due to decreasing distances between the D- and A-unit as indicated in the schematic sketches on the right side. (For interpretation of the references to color in this figure legend, the reader is referred to the web version of this article.)

more flexible linker (two methylene groups) significantly accelerated eT kinetics: While in the system exploiting the semi-rigid linker eT took place in > 10 ns, the flexible linker enabled eT in 20 ps [93].

Conjugation of the linker. The conjugation of the bridge is closely related to its geometrical flexibility: Rigid linkers are almost invariably conjugated and *vice versa*. Generally, photoinduced eT is reported for dyads with both non-conjugated [38,46–48,55,72,82,8577] and conjugated linkers [39–44,49–52,65,68,71,73,75,76,78–82,86–89,91,92,101,106,108]. Using a conjugated linker does not *per se* ensure fast charge separation (<1 ns), as demonstrated for Ru^{II}-NDI (**D2a–*p4p*–A3a**: 100 ns) [72], Ru^{II}-Re^{I} (19 ns, [76]), and porphyrin-POM dyads (*e.g.*, **D1a–*p1p*–A2**: 50 ns) [46,75], for example. However, sub-ns eT is found for both conjugated [38,48,55] and non-conjugated triazole bridged D–A dyads [39–43,47,50–52]. Thus, conjugated triazole linkers do not necessarily lead to more active D–A dyads, nor does the use of rigid linkers. In this context, we would like to point to work by *Odobel et al.*, in which charge separation in rigid and conjugated porphyrin-POM dyads is compared to flexible and non-conjugated dyads (**D1a–*p1p*–A2** *vs.* **D1–*4*–A2**, *cf.* Fig. 5) [75]. While **D1a–*p1p*–A2** does not show any evidence of charge-separation upon photoexcitation of the porphyrin-unit, **D1–*4*–A2** does due to its flexible and non-conjugated linker, which enables through-space eT (see section *Linker flexibility*). Nonetheless, both the flexible and non-conjugated as well as the rigid and conjugated triazole linkers are poor conductors of electronic charge causing slow through-bond eT despite high thermodynamic driving forces.

In some cases, eT across the triazole bridge is even completely blocked, although the process is thermodynamically feasible. These include conjugated and rigid [18,36,37,62,64,67,84,85] as well as non-conjugated and flexible dyads [18,45,56–60,63–66,69]. References that do not report photoinduced eT, draw this conclusion from a comparison of the photophysical properties (*e.g.*, absorption characteristics and photoinduced dynamics) of triazole bridged D–A dyads and reference systems. The latter contain either the respective isolated building blocks (*e.g.*, only the D-moiety or a triazole-substituted D-moiety, see Fig. 1) [18,36,37,64,77,84,85] or dyads in which the triazole bridge has been replaced by a different linker unit (*e.g.*, a phenylene- or alkyne-unit) [18,58,100]. These studies have the excitation of the D-moiety in common. For example, transient absorption studies on Ru^{II}–Co^{III} (**D2c–*p4*–A4**) [85], Ru^{II}–Cu^{II} [86], Ru^{II}–Re^{I} [76], and Ru^{II}–Rh^{III} (**D2a–*p4p*–A5**) [18] dyads (4-connected, conjugated and rigid dyads) reveal the population of a long-lived excited state with excess electron density delocalized across the linker, rather than a charge transfer from the Ru^{II}-ion to the respective acceptor metal center of the dyads. Moreover, for the (semi–)flexible and non-conjugated BODIPY-POM dyad (**D4a–*4*–A2**) time-resolved studies reveal that rapid intersystem crossing or energy transfer processes yield the population of long-lived D-centered triplet states [77].

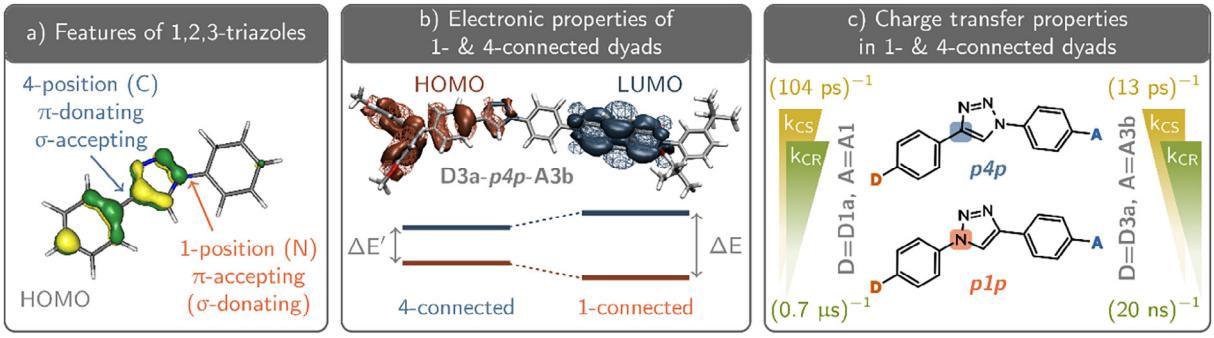

Fig. 6. a) Features of the 1,2,3-triazole linker, *i.e.*, the electron-donating or -accepting property of the triazole, when bound *via* the 4- (blue, *C*-atom) or 1-position (orange, *N*-atom), respectively. Exemplarily, the geometry and HOMO (ρ = ±0.03, *B3LYP/Def2SVP* [109–111]) of a phenylene-triazole-phenylene linker are shown. That the HOMO extends across the triazole and the phenylene moiety attached to the 4-position of the triazole underlines the electronic features of the triazole linker. b) Schematic illustration of the impact of the triazole connectivity on the electronic properties of a respective triazole-bridged D–A dyad [48,55,60]: The electron-accepting character of the triazole when bound *via* the 1-position to the D-unit causes a stabilization of the D-centered HOMO (dark orange) and destabilization of the A-centered LUMO (dark blue) with respect to the 4-connected system. The corresponding D- and A-centered HOMO and LUMO, respectively, obtained by DFT (ρ = ±0.02, *CAM-B3LYP/cc-pVDZ* [115,116]) are shown exemplarily for **D3a**–***p4p***–**A3b**. c) Structural formula of a 4- (***p4p***, top) and 1-connected linker (***p1p***, bottom). Effect of the triazole connectivity on the charge transfer properties at the example of ***p1p***- and ***p4p***-bridged porphyrin-fullerene (**D1a**–**A1**) and TPA-NDI dyads (**D3a**–**A3b**): Generally, the charge separation (k_{CS}, see gold bars) and charge recombination rates (k_{CR}, see green bars) of 4-connected dyads are accelerated compared to their 1-connected counterparts [48,55]. (For interpretation of the references to color in this figure legend, the reader is referred to the web version of this article.)

Similarly, no photoinduced intramolecular eT could be detected with a series of catalytically-active dyads covalently assembling cobalt-based hydrogen-evolving catalysts (see **A4** in Fig. 4 and A7 in Fig. 8) with push–pull organic dyes (see **D3b–CAA** in Fig. 8) [36,37,84]. Although eT from the D- to the A-unit is thermodynamically allowed ($-1.5 < \Delta G^0 < -1.1$ eV) [18,36,37,64,76,77], no charge-separated states are populated in either of these examples. Since upon donor excitation through-bond eT occurs *via* a LUMO-mediated superexchange mechanism (see *Section 3.2*), the absence of charge separation can be rationalized by *i)* high Gibbs free energies for excited state eT ($\Delta G^{\ddagger}$), *ii)* high reorganization energies or *iii)* too weak electronic couplings between the bridge and the D-/A-moieties, respectively.

Triazole connectivity: carbon or nitrogen on the donor side? In the CuAAC reaction, an azide- and an alkyne-substituted unit are clicked together to form a 1,4-disubstituted 1,2,3-triazole ring (*cf.* Fig. 1). Depending on the respective nature of D and A (either azide- or alkyne substituted, see Fig. 1), the triazole bridge can exist in two different constitutional isomers: either the donor moiety is connected to the carbon atom (alkyne-substituted reactant), *i.e.*, at the 4-position of the triazole (4-connected) [36,37,41,43,44, 48,49,52,55,58–60,62,64,67,69,71–73,75–79,82,84–88,93,94,101], or to a nitrogen atom (azide-substituted reactant), *i.e.*, at the 1-position of the triazole (1-connected) [38,42,45–48,50,51,53–55,5 7,60–62,65,66,74,75,81,89,92,113,114]. One of the main reasons for selecting a specific isomer is certainly the synthetic accessibility of azide- and alkyne-substituted molecules that are linked together and thus determine the constitution of the triazole bridge. For example, there are only few examples of $[Ru(bpy)_3]^{2+}$-type complexes that have been successfully functionalized with azide-groups [26,92,113,114] and subsequently used in a CuAAC CLICK reaction [42,45,89,92], notably because of the instability of the azide-group which can be sensitive to heat, shock, and water [23,72]. As a consequence, most of the dyads based on Ru^{II} polypyridyl donor units (**D2**) are 4-connected [44,52,67,71, 72,76,85–88, 94]. Compared to these discrepancies for dyads with Ru^{II} polypyridyl-like donors, the literature is balanced around triazole-bridged dyads bearing 1- [38,46,48,50, 51,57,60–62,65,66 ,74,75,81] and 4-connected [41,48,49,59,60,62,64, 69,73,75,78,79, 82] porphyrin donor units (**D1**), respectively.

Currently, the sole systematic studies comparing the properties of the two triazole constitutional isomers (1- and 4-connected dyads) rely on a series of porphyrin-fullerene (see units **D1a** and **A1** in Fig. 2) [48,60] and TPA-NDI dyads (see units **D3a** and **A3b** in Fig. 2) [55]. The studies investigate the influence of the triazole connectivity for D-A dyads bearing rigid and conjugated phenylene-triazole-phenylene linkers, i.e., ***p4p*** and ***p1p*** [48,55,60] (see Fig. 6c), as well as *e.g.*, ***m4m***, ***p1m***, or ***p4m*** [48,60] (see Fig. 4b). 4-connected triazoles were found to act as electron-donating groups, while 1-connected triazoles act as electron-withdrawing groups. This is reflected in a higher oxidation potential of the D-unit in D-A dyads in which the D-unit is bonded to the 4-position instead of the 1-position of the triazole bridge [48,55]. This stems from the delocalization of the lone pair of the nitrogen atom into the triazole π-system (*cf.* Fig. 6a), ultimately lowering the electron-donating ability, i.e., the positive mesomeric effect (*+M*−effect), of the donor moiety when connected to the 4-position of the triazole. This causes a destabilization of the D-centered HOMO and a stabilization of the A-centered LUMO, in 4- with respect to 1-connected systems (*cf.* Fig. 6a and Fig. 4b). For instance, the HOMO-LUMO gap (measured between the D-centered HOMO and A-centered LUMO) of **D1a–*p4p*–A1** is 0.02 eV smaller than that of **D1a–*p1p*–A1** [48]. Moreover, *De Miguel et al.* identified the charge separation rate in **D1a-A1** dyads to be three times higher when the porphyrin is linked to the 4- than to the 1-position of the triazole [48]. This is due to the lower HOMO-LUMO gap in the 4-connected systems and therefore the lower driving force for the LUMO-mediated superexchange eT. This is caused by a favorable influence of electron-donating and -withdrawing effects on the D- and A-units, respectively. However, for the studied systems charge recombination falls into the Marcus inverted region [48,55]. Consequently, the lower HOMO–LUMO gap causes a slightly faster charge recombination (*e.g.*, 667 *vs.* 833 ns for **D1a–*p4p*–A1** *vs.* **D1a–*p1p*–A1**, or 417 *vs.* 667 ns **D1a–*p4m*–A1** *vs.* **D1a–*p1m*–A1**) [48]. Similarly, the charge recombination rate of the **D3a–*p4p*–A3b** (7 ns) is higher than for the **D3a–*p1p*–A3b** dyad (20 ns, see Fig. 6c) [55].

In summary, the fraction of literature reporting evidence for light-driven eT across the triazole bridge does not seem to indicate a functional preference for either of the isomers [38,41–45,49–52 ,55,65,73–75,78,79,81,82,86,101]. However, there is an apparent difference when considering the bridges facilitating sub-ns eT [38,42,43,45,46,49–52,55]: such fast processes are more often observed for 1-connected systems [38,42,45,46,50,51,55]. This seems counter-intuitive with respect to the connectivity factors: Due to the higher HOMO-LUMO gap the thermodynamic driving

force of eT (ΔG^0) is smaller in 1- with respect to 4-connected dyads. However, the observed trend might also be a result of the different donor units that were predominantly used: While many 1-connected dyads utilize the rather high-performing porphyrins as donors [38,46,50,51,55,80], a substantial amount of 4-connected dyads contained Ru^{II} polypyridyl donors, which generally do not show fast eT across triazole bridges [43,52,67,72,86,107].

3.2. Oxidative vs. reductive photoinduced eT

Most triazole-bridged D-A dyads reported in the literature utilize a photoactive electron donor (D-moiety). However, this is not necessarily the most suited architecture to ensure, *e.g.*, high charge-separation rates and the population of long-lived charge-separated states. For rigid and conjugated systems [18,38,46,48,49,55,57,62,64,67,72,76,82,89], such as **D1a–*p4p*–A1** or **D3a–*p4p*–A3b** (see Fig. 6c), only a few examples show excited state eT upon photoexcitation of the donor (oxidative photoinduced eT ↔ oxidation of the light-absorbing D-unit) [38,46,48,49,55,72,76,82]. On the other hand, all these systems show eT upon photoexcitation of the A-unit (reductive photoinduced eT ↔ reduction of the light-absorbing A-unit) [46,55,89]. In addition, while only a minority of donor-excited dyads (rigid and conjugated linkers) are capable of undergoing eT on a sub-ns timescale [38,48,51], almost all the dyads with rigid and all with conjugated linkers do so upon excitation of the acceptor [46,55].

In this context the rigid and conjugated porphyrin-NDI and TPA-NDI dyads, namely **D1b–*p1p*–A3a** and **D3a–*p4p*–A3b** (*cf.* Fig. 6b) [46,55] are noteworthy: In these dyads both the A- and D-moieties are photoactive (*e.g.*, absorb between 300 and 600 nm). Hence, they served as the basis for systematic studies of the charge transfer properties after selective excitation of the D- or A-unit [46,55]. These studies allow insights into the differences between light-induced hT and eT across the triazole bridge: Upon photoexcitation of the D-unit of **D1b–*p1p*–A3a,** *Odobel* and co-workers [46] observed a quenching process with a characteristic time-constant of 9 ns. This was associated with excited state eT from the singlet state since electron transfer from the triplet state has an insufficient driving force. The accumulation of significant amounts of charge-separated states was not observed, as, according to Marcus theory, the recombination of charges should occur much faster than charge separation. However, if the A-unit is excited, the picture changes completely: Upon A-excitation about 90% of the photoexcited NDI singlet states decay with a characteristic rate of 14 ps. This process has been identified as hT from the photoexcited NDI to the porphyrin unit. The remaining 10% of the photoexcited ^{1}NDI* states undergo intersystem crossing, populating ^{3}NDI states, followed by hT to **D1b**. Notably, the resulting charge-separated triplet state shows a comparably long lifetime (90 ns) due to the spin-forbidden nature of charge recombination. Similarly, photoexcitation of the NDI-unit of **D3a–*p4p*–A3b** is followed by ultrafast charge transfer (2 ps), *i.e.*, hT from the photoexcited NDI towards the **A3b**-unit [55]. As a single exception, the charge separation observed for a 1-connected Ru^{II}-tryptophan dyad upon excitation of the tryptophan acceptor moiety is comparably slow (3 μs) [89]. Nevertheless, this is consistent with the generally slower excited-state eT reactivities observed for triazole-bridged dyads with Ru^{II} donors [71,72,86–89], especially in comparison to a respective bimolecular system (intermolecular eT) [76].

The differences between the charge transfer properties can be rationalized considering the underlying mechanisms, which in first approximation are based on the relative energies of donor-, bridge-, and acceptor-centered molecular orbitals (see Fig. 7):

- Upon photoexcitation of the D-unit, eT occurs *via* LUMO-mediated superexchange, *i.e.*, through orbital mixing of unoccupied orbitals, where the triazole bridge-centered π*-orbitals are higher in energy than the respective π*-orbitals that are populated upon photoexcitation (*e.g.*, upon ππ* or metal-to-ligand charge-transfer absorption) [95]. This means that the energy barrier posed by the triazole determines if and how fast electron transfer takes place. This leads to slow rates or rather to the hindrance of eT across the triazole bridge with an increasing energy of the triazole-centered π*-orbital [18,46,55,57,58,64,70,75,77]. The energy of the triazole-centered π*-orbital determines the Gibbs free energy for the formation of the triazole-centered transition state ($\Delta G^{\ddagger}$), which can be significant. For example, $\Delta G^{\ddagger}$ in a Ru^{II}–Rh^{III} (**D2a–*p4p*–A5**, [18]), a porphyrin-Co^{III} (**COOH-Ph–*p*–D1b–*p4*–A4** [64]), or a BODIPY-POM (**D4a–*4*–A2** [77]) dyad was found to be high enough that through-bond eT was shut down completely. Instead, long-lived triplet states with excess electron density in proximity to the D-moiety are populated [18,64,77].
- When the A-moiety is photoexcited, charge-transfer occurs *via* hT since the bridge-centered MO lies energetically between the D- (HOMO) and A-centered MOs. Since hT is a fully energetically downhill process, the charge-transfer processes are faster compared to LUMO-mediated superexchange when exciting the D-unit [95].

In addition, the connectivity of the triazole influences the dynamics of the charge transfer processes: In fully-conjugated dyads the A-centered LUMO is destabilized [48] when the donor is linked to the 1- compared to the 4-position (*cf. Section 3.1* and Fig. 6b). Thus, the free enthalpy for an excited state eT ($\Delta G^{\ddagger}$) is higher in 4-connected dyads compared to their 1-connected counterparts. This causes higher charge-separation rates (k_{CS}) for 4- than for 1-connected systems [48,55] (*e.g.*, k_{CS} is 9.6 or 5.5 ns^{-1} for **D1a–*p4p*–A1** or **D1a–*p1p*–A1**, respectively [48]). *Vice versa*, it can be expected that hT is faster in 4- than in 1-connected systems: The 4-connection causes a destabilization of the D-centered HOMO with respect to the 1-connected counterpart [48]. This leads to a higher driving force for the hT process (ΔG^0) in the 4- compared to the 1-connected dyads. This trend is confirmed by the present studies on **D3a–*p4p*–A3b** (k_{CS} = 0.5 ps^{-1}) and **D1b–*p1p*–A3a** (k_{CS} = 0.1 ps^{-1}). Nevertheless, both dyads bear different D-units (triphenylamine *vs.* Zn^{II} porphyrin) [46,55]. To date, however, there are no systematic studies in which only the triazole linkage is varied, while all other structural and electronic parameters are held constant.

In summary, upon photoexciting the D-unit, LUMO-mediated superexchange eT occurs, with the energy barrier of the eT being determined by the relative position of the π*-orbitals of the triazole bridge [95]. This barrier ($\Delta G^{\ddagger}$) makes the triazole linker a poor conductor of electronic charge, hindering through-bond eT despite a high thermodynamic driving force (ΔG^0) [38,46,48,49,55,72,76,82]. However, for the systems which do not show photoinduced oxidative eT, photoinduced reductive eT was observed following excitation of the A-moiety [46,55,89]. The latter process is based on HOMO-mediated hT. This mechanism is found to be much faster than the oxidative eT in triazole-bridged dyads, which is reflected in comparably fast charge separation (1 ps < τ_{CS} < 20 ps) [46,55]. The absence of photoinduced eT upon D-excitation is observed in many dyads with different D- and A-moieties, namely Ru^{II} complex [18], BODIPY [58] or porphyrin [56,59,63,65,66] as D- and Rh^{III} complex [18], fullerene [59], organic dye [56,63], or porphyrin [58,65,66] as A-unit. Consequently, two inherent characteristics for the triazole bridges impact the electron transfer rates in D-A dyads: Triazoles are poor charge conductors in through-bond eT upon D-excitation (high

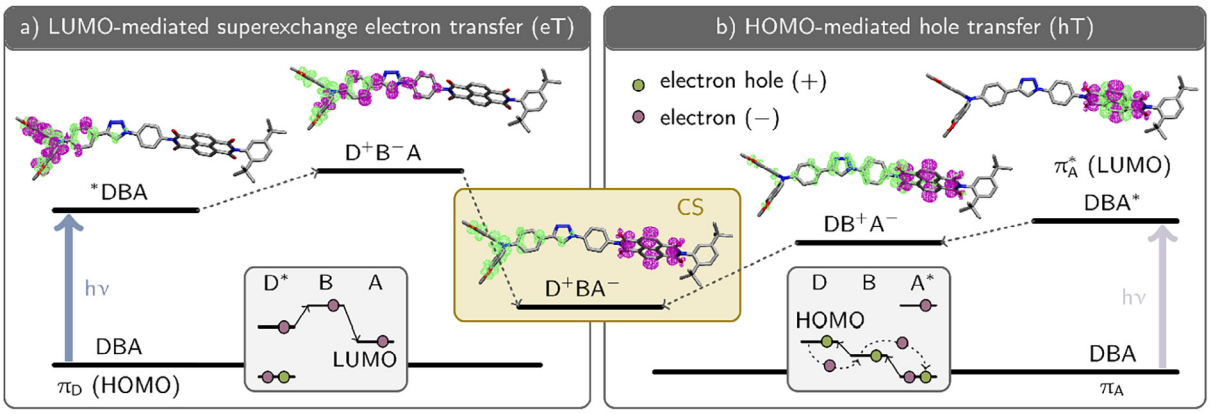

Fig. 7. Schematic representation of the charge transfer mechanisms that occur upon excitation of the D- (a, LUMO-mediated superexchange eT) or A-unit (b, HOMO-mediated hT). For illustration, the origin and excess electron density of the **D1b**–***p1p***–**A3a** dyad are shown in green (occupied π-orbitals) and violet (unoccupied π*-orbitals), respectively. All shown molecular orbitals were obtained at the TD-DFT level of theory (ρ = ±0.01, *CAM-B3LYP/cc-pVDZ* [115,116]). The figure presents specific molecular example for the more general concept depicted in Fig. 3. (For interpretation of the references to color in this figure legend, the reader is referred to the web version of this article.)

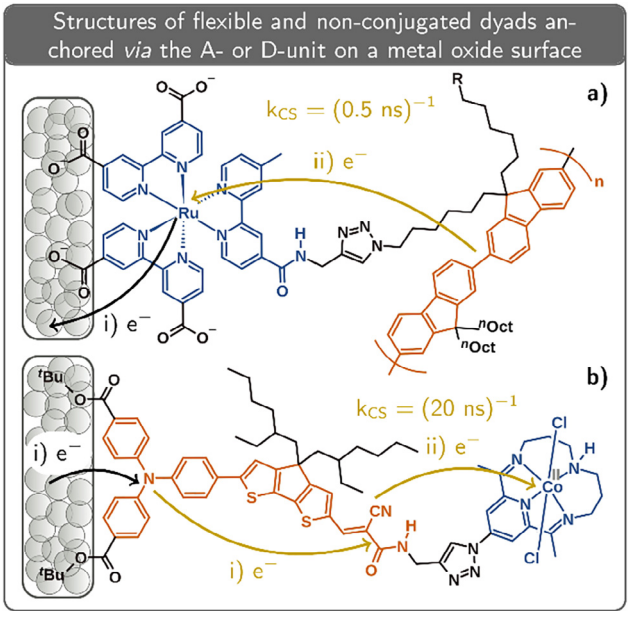

Fig. 8. Structural formulas of the polyfluorene-Ru^{II} (a, **D5**–***1***–**A6**) and TPA-cyanoacrylamide(CAA)-Co^{III} triad (b, **D3b**–**CAA**–***4***–**A7**) and summary of the photoinduced charge transfer processes upon photoexcitation of the Ru^{II}-chromophore or the TPA-CAA push-pull dye anchored on TiO_2 (a) or NiO (b), respectively [52,84]. The intramolecular (k_{CS}) and intermolecular (between dyad and metal oxide) eT processes are indicated by gold and black arrows, respectively. In case of **D3b**–**CAA**–***4***–**A7**, excess electron density is shifted from the TPA to the CAA moiety upon light-absorption, followed by a sub-ps hole injection into the NiO substrate, i.e., reductive quenching of the photo-oxidized TPA moiety. Subsequently, a thermal CAA-to-Co^{II} (**CAA**-to-**A7**) eT occurs. Note that the acceptor was electrochemically reduced from the Co^{III} to the Co^{II} oxidation state prior to excitation.

$\Delta G^{\ddagger}$) but allow fast charge separation *via* a hT mechanism, *i.e.*, photoexcitation of the A-unit.

3.3. Excited state vs. ground state eT

While photoinduced intramolecular eT has been studied for most triazole-linked D-A dyads, thermal eT, i.e., eT in the electronic ground state of reduced or oxidized assemblies, has been studied only occasionally (see also Fig. 3 and section 1 for introductory remarks). The vast majority reports of thermally activated eT concerns dyads with Ru^{II} polypyridyl-type as donor- or acceptor-unit (*e.g.*, **D2a**, see Fig. 2a) [52,71,72,86–89,92,94]. For instance, *Aukauloo et al.* attached a Ru^{II}-chromophore to several electron donors, such as tryptophan, tyrosine, as well as Ni^{II}- and Fe^{II}-complexes, or acceptors, *e.g.*, NDI, Ni^{II}- and Re^{I}-complex [71,72,76,87–89,92,94]. In their experiments, the excited state of the photosensitizer is quenched by a sacrificial electron donor or acceptor yielding the reduced or oxidized species of the photoactive unit, respectively. Subsequently, eT takes place to or from the secondary unit of the dyad. The authors report on thermally activated eT on the ns to μs timescale (between 20 ns and 31 μs), i.e., slower than excited state eT, which can occur on the sub-ns timescale [38,41,48,50,51,75,80,93]. While especially in dyads with Ru^{II} donors no excited state eT across the triazole bridge was observed [18,37,76,85], the studies of *Aukauloo et al.* reveal thermal eT across a triazole bridge. From this, the following mechanistic conclusions can be drawn: *i)* $\Delta G^{\ddagger}$ for eT is smaller, *ii)* the reorganization energy is smaller, and/or *iii)* the eT driving force (ΔG^{0}) is higher for formally reduced/oxidized dyads compared to the unmodified dyads in the excited state. However, not only thermodynamic considerations are important, but also kinetic factors have to be taken into account. In particular, the molecular species resulting from oxidation/reduction of the photoactive center are generally longer lived that the excited-states of the respective photoactive units. Hence, a larger temporal window is available for subsequent charge transfer processes from the photoactive to the catalytically active unit.

Currently, the only system known to us in which thermally activated eT occurs across a triazole bridge on the sub-ns time scale is a polyfluorene-Ru^{II} system (**D5**–***1***–**A6**) anchored on TiO_2 (see Fig. 8a) introduced by *Schanze* and co-workers [52]. In this dyad, the photoexcited *Ru^{II} moieties bound to the metal oxide rapidly inject electrons into the conduction band of TiO_2 (<1 ps, see black arrow in Fig. 8a) forming Ru^{III}-units. Subsequently, eT from the polyfluorene polymer backbone to the oxidized Ru^{III} occurs within 0.5 ns (see gold arrow in Fig. 8a). The fast charge transfer is due to the flexible polymer structure, which allows for sub-ns charge transfer processes [40,42,43,45] (see section 3.1, *Linker flexibility*). With respect to the polymeric systems that show sub-ns excited state eT (between 1 and 200 ps) [40,42,43,45], the thermal eT in **D5**–***1***–**A7** is quite slow [52].

Another dyad that only shows thermal eT is composed of a TPA-cyanoacrylamide (CAA) push-pull dye (**D3b-CAA**, see Fig. 8b) and a Co complex acceptor (**A7**, see Fig. 8b). When **D3b**–**CAA**–***4***–**A7** in solution (**A7** in the Co^{III} oxidation state) is electronically excited

in the absence of electron donors no photoinduced eT is observed. This is apparent from the absence of any spectral features pointing to the formation of the reduced acceptor. Instead, a long-lived triplet state with excess electron density on the cyanoacrylate (CAA) moiety of **D3b–CAA** is formed within 150 ps [36]. A similar dyad, **D3c–CAA–*4*–A4** (with **D3c** corresponding to the **D3b**-unit without the cyclopentadithiophene substituent), also showed no intramolecular photoinduced eT in solution irrespective of the initial **A4** oxidation state [37]. When **D3b–CAA–*4*–A7** is bound to NiO *via* the TPA-moiety [84], ultrafast hole injection (<1 ps) is observed upon photoexcitation of the push-pull dye (**D3b–CAA**, see black arrow in Fig. 8b). This yields a singly-reduced CAA-moiety. Application of a reductive potential to the film extends the lifetime of the reduced CAA and reduces **A7** to the Co^{II} state prior to excitation. Under these conditions, hole injection is followed by eT to **A7**, forming a Co^{I}-center within 20 ns (see gold arrow in Fig. 8b). This intramolecular eT occurs biphasic with the two characteristic time constants <20 ns and 9 μs [84]. This is due to conformational gating of eT, indicating that the flexible linker structure allows the dyad to sample a conformational space until an intramolecular geometry optimal for eT to take place is acquired. Consequently, the intramolecular, thermal eT in **D3b–CAA–*4*–A7** is slower than in **D5–*1*–A6**, where the geometry is primarily determined by the polymer structure [52,84].

The systems mentioned in this section exclusively show thermal eT, *i.e.*, eT in the electronic ground state, while no eT occurs in the absence of electron donors/acceptors. In the examples, electron transfer from/to the dyad by sacrificial agents quenches the photoexcited moiety, yielding a reduced [84] or oxidized species [52]. The absence of photoinduced eT is attributed to its competition with other deactivation processes, such as relaxation back to the ground state [52,84] or the population of bridge-centered states [84]. If these processes occur faster than charge separation, no excited state eT is observed. This can even be the case for dyads that have excited state lifetimes of hundreds of ns, such as Ru^{II} complexes. If, however, the excited state is quenched rapidly, then the reduced or oxidized species can be long-lived enough to enable eT.

4. Conclusion

CLICK chemistry presents an attractive approach to connect important functional molecular building blocks. However, the resulting triazoles are by no means innocent with respect to the desired overall function of, *e.g.,* the targeted molecular dyad. The role of triazole-CLICK bridges in intramolecular, photoinduced electron transfer (eT) processes in donor-bridge-acceptor (D–A) dyads is complex: On one hand, these eT processes depend on the structural (*flexibility* and *conjugation*) and electronic properties (*connectivity*) of the triazole bridge, which determine if through-bond or through-space eT occurs (donor-acceptor, d_{DA}) as well as the energy barrier ($\Delta G^{\ddagger}$) and driving force of the eT (ΔG^{0}). On the other hand, the eT processes also rely on structural factors determined by the D- and A-moieties, such as the electronic coupling of the D- and A-units to each other and to the triazole bridge, respectively, as well as on mechanistic factors. In the latter case, it is differentiated whether the electron transfer follows the excitation of the donor (LUMO-mediated superexchange eT) or the acceptor (HOMO-mediated hT).

This review highlighted specific examples selected from the literature on eT in triazole-bridged D–A systems to demonstrate the factors associated with triazole bridges in relation to photoinduced charge transfer processes. Specifically: *i)* the ability to control eT rates through the flexibility and conjugation of the triazole linker (*Section 3.1*) *ii)* the possibility to influence the relative energy of the occupied D- and unoccupied A-molecular orbitals *via* the connectivity (*Section 3.1*), *iii)* the poor conductivity of triazole bridges in LUMO-mediated superexchange eT (reductive excited state eT, *Section 3.2*), iv) the possibility to enable fast charge transfer *via* oxidative excited state eT (HOMO-mediated hT, *Section 3.2*), and v) the ability to obtain diffusion-limited charge separation through thermally activated eT after quenching of the photoexcited dyad (*Section 3.3*) was shown.

To this end, the following criteria can be derived for the design of triazole-bridged D-A dyads with emphasis on electron transfer properties:

- The **charge-separation rate (k_{CS})** but also the **charge-recombination rate (k_{CR})** is higher for dyads with flexible linkers (through-space eT). However, the **charge-recombination rate (k_{CR})** is lower for rigid dyads (through-bond eT)**.**
- The **energy barrier ($\Delta G^{\ddagger}$)** for oxidative is higher than for reductive photoinduced eT. Thus, triazoles (irrespective of connectivity, flexibility, and conjugation) are poor conductors of electronic charge upon donor excitation resulting in low **charge-separation rates (k_{CS})** or even a kinetical hindrance of through-bond eT.
- The **charge-separation rate (k_{CS})** for reductive photoinduced eT (acceptor excitation) is higher in 1- compared to 4-connected dyads.
- The **driving force for eT (ΔG^{0})** is higher in 4- than in 1-connected dyads irrespective of the linker flexibility and conjugation.

Data availability

Data will be made available on request.

Declaration of Competing Interest

The authors declare that they have no known competing financial interests or personal relationships that could have appeared to influence the work reported in this paper.

Acknowledgements

Funding by the Deutsche Forschungsgemeinschaft (German Research Foundation) *via* the SFB-TRR CATALIGHT (project number: 364549901, TRR234, sub-project: A1) and by the French National Research Agency in the framework of the "Investissements d'avenir" program (ANR-15-IDEX-02, Labex ARCANE, and CBH-EUR-GS, ANR-17-EURE-0003) are gratefully acknowledged. S.B. wants to thank the Franco-German University for the cotutelle thesis funding support. All high-performance calculations were performed at the Universitätsrechenzentrum of the Friedrich Schiller University Jena.

References

[1] V. Balzani (Ed.), Electron Transfer in Chemistry, Wiley, 2001, https://doi.org/10.1002/9783527618248.
[2] A.J. Esswein, D.G. Nocera, Hydrogen Production by Molecular Photocatalysis, Chem. Rev. 107 (2007) 4022–4047, https://doi.org/10.1021/cr050193e.
[3] G. Knör, Recent progress in homogeneous multielectron transfer photocatalysis and artificial photosynthetic solar energy conversion, Coord. Chem. Rev. 304–305 (2015) 102–108, https://doi.org/10.1016/j.ccr.2014.09.013.
[4] D.R. Whang, D.H. Apaydin, Artificial Photosynthesis: Learning from Nature, ChemPhotoChem. 2 (2018) 148–160, https://doi.org/10.1002/cptc.201700163.
[5] Y. Hou, X. Zhang, K. Chen, D. Liu, Z. Wang, Q. Liu, J. Zhao, A. Barbon, Charge separation, charge recombination, long-lived charge transfer state formation and intersystem crossing in organic electron donor/acceptor dyads, J. Mater. Chem. C. 7 (2019) 12048–12074, https://doi.org/10.1039/C9TC04285G.

[6] C.S. Ponseca, P. Chábera, J. Uhlig, P. Persson, V. Sundström, Ultrafast Electron Dynamics in Solar Energy Conversion, Chem. Rev. 117 (16) (2017) 10940–11024.
[7] T.H. Bürgin, O.S. Wenger, Recent Advances and Perspectives in Photodriven Charge Accumulation in Molecular Compounds: A Mini Review, Energy & Fuels. 35 (2021) 18848–18856, https://doi.org/10.1021/acs.energyfuels.1c02073.
[8] L. Hammarström, Accumulative Charge Separation for Solar Fuels Production: Coupling Light-Induced Single Electron Transfer to Multielectron Catalysis, Acc. Chem. Res. 48 (2015) 840–850, https://doi.org/10.1021/ar500386x.
[9] A. Pannwitz, O.S. Wenger, Proton-coupled multi-electron transfer and its relevance for artificial photosynthesis and photoredox catalysis, Chem. Commun. 55 (2019) 4004–4014, https://doi.org/10.1039/C9CC00821G.
[10] S. Rau, D. Walther, J.G. Vos, Inspired by nature: light driven organometallic catalysis by heterooligonuclear Ru(ii) complexes, Dalt. Trans. (2007) 915, https://doi.org/10.1039/b615987g.
[11] H. Ozawa, M. Haga, K. Sakai, A Photo-Hydrogen-Evolving Molecular Device Driving Visible-Light-Induced EDTA-Reduction of Water into Molecular Hydrogen, J. Am. Chem. Soc. 128 (2006) 4926–4927, https://doi.org/10.1021/ja058087h.
[12] P. Lei, M. Hedlund, R. Lomoth, H. Rensmo, O. Johansson, L. Hammarström, The Role of Colloid Formation in the Photoinduced H 2 Production with a Ru II −Pd II Supramolecular Complex: A Study by GC, XPS, and TEM, J. Am. Chem. Soc. 130 (2008) 26–27, https://doi.org/10.1021/ja0776780.
[13] A.F. Heyduk, D.G. Nocera, Hydrogen Produced from Hydrohalic Acid Solutions by a Two-Electron Mixed-Valence Photocatalyst, Science 293 (5535) (2001) 1639–1641.
[14] A. Fihri, V. Artero, M. Razavet, C. Baffert, W. Leibl, M. Fontecave, Cobaloxime-Based Photocatalytic Devices for Hydrogen Production, Angew. Chemie Int. Ed. 47 (2008) 564–567, https://doi.org/10.1002/anie.200702953.
[15] G.-G. Luo, Z.-H. Pan, J.-Q. Lin, D. Sun, Tethered sensitizer–catalyst noble-metal-free molecular devices for solar-driven hydrogen generation, Dalt. Trans. 47 (2018) 15633–15645, https://doi.org/10.1039/C8DT02831A.
[16] M. Schulz, M. Karnahl, M. Schwalbe, J.G. Vos, The role of the bridging ligand in photocatalytic supramolecular assemblies for the reduction of protons and carbon dioxide, Coord. Chem. Rev. 256 (2012) 1682–1705, https://doi.org/10.1016/j.ccr.2012.02.016.
[17] K.L. Mulfort, L.M. Utschig, Modular Homogeneous Chromophore-Catalyst Assemblies, Acc. Chem. Res. 49 (2016) 835–843, https://doi.org/10.1021/acs.accounts.5b00539.
[18] L. Zedler, P. Wintergerst, A.K. Mengele, C. Müller, C. Li, B. Dietzek-Ivanšić, S. Rau, Outpacing conventional nicotinamide hydrogenation catalysis by a strongly communicating heterodinuclear photocatalyst, Nat. Commun. 13 (2022) 2538, https://doi.org/10.1038/s41467-022-30147-4.
[19] A.B. Ricks, G.C. Solomon, M.T. Colvin, A.M. Scott, K. Chen, M.A. Ratner, M.R. Wasielewski, Controlling electron transfer in donor-bridge-acceptor molecules using cross-conjugated bridges, J. Am. Chem. Soc. 132 (2010) 15427–15434, https://doi.org/10.1021/ja107420a.
[20] D.E. Stasiw, J. Zhang, G. Wang, R. Dangi, B.W. Stein, D.A. Shultz, M.L. Kirk, L. Wojtas, R.D. Sommer, Determining the Conformational Landscape of σ and π Coupling Using para -Phenylene and "Aviram–Ratner" Bridges, J. Am. Chem. Soc. 137 (2015) 9222–9225, https://doi.org/10.1021/jacs.5b04629.
[21] Z. Jin, Y.C. Teo, N.G. Zulaybar, M.D. Smith, Y. Xia, Streamlined Synthesis of Polycyclic Conjugated Hydrocarbons Containing Cyclobutadienoids via C-H Activated Annulation and Aromatization, J. Am. Chem. Soc. 139 (2017) 1806–1809, https://doi.org/10.1021/jacs.6b12888.
[22] B. Pelado, F. Abou-Chahine, J. Calbo, R. Caballero, P. de la Cruz, J.M. Junquera-Hernández, E. Ortí, N.V. Tkachenko, F. Langa, Role of the Bridge in Photoinduced Electron Transfer in Porphyrin-Fullerene Dyads, Chem. – A Eur. J. 21 (2015) 5814–5825, https://doi.org/10.1002/chem.201406514.
[23] N. Zabarska, A. Stumper, S. Rau, CuAAC click reactions for the design of multifunctional luminescent ruthenium complexes, Dalt. Trans. 45 (2016) 2338–2351, https://doi.org/10.1039/C5DT04599A.
[24] P. Kautny, D. Bader, B. Stöger, G.A. Reider, J. Fröhlich, D. Lumpi, Structure-Property Relationships in Click-Derived Donor-Triazole-Acceptor Materials, Chem. – A Eur. J. 22 (2016) 18887–18898, https://doi.org/10.1002/chem.201603510.
[25] H.C. Kolb, M.G. Finn, K.B. Sharpless, Click Chemistry: Diverse Chemical Function from a Few Good Reactions, Angew. Chemie – Int. Ed. 40 (2001) 2004–2021, https://doi.org/10.1002/1521-3773(20010601)40:11<2004::AID-ANIE2004>3.0.CO;2-5.
[26] E.C. Constable, C.E. Housecroft, J.R. Price, L. Schweighauser, J.A. Zampese, First example of a CLICK reaction of a coordinated 4′-azido-2,2′:6′,2″-terpyridine ligand, Inorg. Chem. Commun. 13 (2010) 495–497, https://doi.org/10.1016/j.inoche.2010.01.019.
[27] V.V. Rostovtsev, L.G. Green, V.V. Fokin, K.B. Sharpless, A Stepwise Huisgen Cycloaddition Process: Copper(I)-Catalyzed Regioselective "Ligation" of Azides and Terminal Alkynes, Angew. Chemie Int. Ed. 41 (2002) 2596–2599, https://doi.org/10.1002/1521-3773(20020715)41:14<2596::AID-ANIE2596>3.0.CO;2-4.
[28] Y. Hua, A.H. Flood, Click chemistry generates privileged CH hydrogen-bonding triazoles: the latest addition to anion supramolecular chemistry, Chem. Soc. Rev. 39 (2010) 1262, https://doi.org/10.1039/b818033b.
[29] J. Lauko, P.H.J. Kouwer, A.E. Rowan, 1 H -1,2,3-Triazole: From Structure to Function and Catalysis, J. Heterocycl. Chem. 54 (2017) 1677–1699, https://doi.org/10.1002/jhet.2770.
[30] D. Schweinfurth, L. Hettmanczyk, L. Suntrup, B. Sarkar, Metal Complexes of Click-Derived Triazoles and Mesoionic Carbenes: Electron Transfer, Photochemistry, Magnetic Bistability, and Catalysis, Zeitschrift Für Anorg. Und Allg, Chemie. 643 (2017) 554–584, https://doi.org/10.1002/zaac.201700030.
[31] B. Schulze, U.S. Schubert, Beyond click chemistry – supramolecular interactions of 1,2,3-triazoles, Chem. Soc. Rev. 43 (2014) 2522, https://doi.org/10.1039/c3cs60386e.
[32] T.L. Mindt, H. Struthers, L. Brans, T. Anguelov, C. Schweinsberg, V. Maes, D. Tourwé, R. Schibli, "Click to Chelate": Synthesis and Installation of Metal Chelates into Biomolecules in a Single Step, J. Am. Chem. Soc. 128 (2006) 15096–15097, https://doi.org/10.1021/ja066779f.
[33] S. Lee, Y. Hua, H. Park, A.H. Flood, Intramolecular Hydrogen Bonds Preorganize an Aryl-triazole Receptor into a Crescent for Chloride Binding, Org. Lett. 12 (2010) 2100–2102, https://doi.org/10.1021/ol1005856.
[34] Y. Liu, A. Sengupta, K. Raghavachari, A.H. Flood, Anion Binding in Solution: Beyond the Electrostatic Regime, Chem. 3 (2017) 411–427, https://doi.org/10.1016/j.chempr.2017.08.003.
[35] N. Li, P. Zhao, N. Liu, M. Echeverria, S. Moya, L. Salmon, J. Ruiz, D. Astruc, "Click" Chemistry Mildly Stabilizes Bifunctional Gold Nanoparticles for Sensing and Catalysis, Chem. – A Eur. J. 20 (2014) 8363–8369, https://doi.org/10.1002/chem.201402652.
[36] S. Bold, T. Straistari, A.B. Muñoz-García, M. Pavone, V. Artero, M. Chavarot-Kerlidou, B. Dietzek, Investigating Light-Induced Processes in Covalent Dye-Catalyst Assemblies for Hydrogen Production, Catalysts. 10 (2020) 1340, https://doi.org/10.3390/catal10111340.
[37] S. Bold, L. Zedler, Y. Zhang, J. Massin, V. Artero, M. Chavarot-Kerlidou, B. Dietzek, Electron transfer in a covalent dye–cobalt catalyst assembly – a transient absorption spectroelectrochemistry perspective, Chem. Commun. 54 (2018) 10594–10597, https://doi.org/10.1039/C8CC05556D.
[38] V. Nikolaou, F. Plass, A. Planchat, A. Charisiadis, G. Charalambidis, P.A. Angaridis, A. Kahnt, F. Odobel, A.G. Coutsolelos, Effect of the triazole ring in zinc porphyrin-fullerene dyads on the charge transfer processes in NiO-based devices, Phys. Chem. Chem. Phys. 20 (2018) 24477–24489, https://doi.org/10.1039/C8CP04060E.
[39] R. Schroot, T. Schlotthauer, B. Dietzek, M. Jäger, U.S. Schubert, Extending Long-lived Charge Separation Between Donor and Acceptor Blocks in Novel Copolymer Architectures Featuring a Sensitizer Core, Chem. – A Eur. J. 23 (2017) 16484–16490, https://doi.org/10.1002/chem.201704180.
[40] Z.A. Morseth, T.V. Pho, A.T. Gilligan, R.J. Dillon, K.S. Schanze, J.R. Reynolds, J.M. Papanikolas, Role of Macromolecular Structure in the Ultrafast Energy and Electron Transfer Dynamics of a Light-Harvesting Polymer, J. Phys. Chem. B. 120 (2016) 7937–7948, https://doi.org/10.1021/acs.jpcb.6b05589.
[41] T.H. Ngo, D. Zieba, W.A. Webre, G.N. Lim, P.A. Karr, S. Kord, S. Jin, K. Ariga, M. Galli, S. Goldup, J.P. Hill, F. D'Souza, Engaging Copper(III) Corrole as an Electron Acceptor: Photoinduced Charge Separation in Zinc Porphyrin-Copper Corrole Donor-Acceptor Conjugates, Chem. – A Eur. J. 22 (2016) 1301–1312, https://doi.org/10.1002/chem.201503490.
[42] L. Wang, E. Puodziukynaite, E.M. Grumstrup, A.C. Brown, S. Keinan, K.S. Schanze, J.R. Reynolds, J.M. Papanikolas, Ultrafast Formation of a Long-Lived Charge-Separated State in a Ru-Loaded Poly(3-hexylthiophene) Light-Harvesting Polymer, J. Phys. Chem. Lett. 4 (2013) 2269–2273, https://doi.org/10.1021/jz401089v.
[43] H. Shi, L. Du, W. Xiong, M. Dai, W.K. Chan, D.L. Phillips, Study of electronic interactions and photo-induced electron transfer dynamics in a metalloconjugated polymer–single-walled carbon nanotube hybrid by ultrafast transient absorption spectroscopy, J. Mater. Chem. A. 5 (2017) 18527–18534, https://doi.org/10.1039/C7TA02753B.
[44] E. Puodziukynaite, L. Wang, K.S. Schanze, J.M. Papanikolas, J.R. Reynolds, Poly (fluorene-co-thiophene)-based ionic transition-metal complex polymers for solar energy harvesting and storage applications, Polym. Chem. 5 (2014) 2363, https://doi.org/10.1039/c3py01582c.
[45] L. Wang, E. Puodziukynaite, R.P. Vary, E.M. Grumstrup, R.M. Walczak, O.Y. Zolotarskaya, K.S. Schanze, J.R. Reynolds, J.M. Papanikolas, Competition between Ultrafast Energy Flow and Electron Transfer in a Ru(II)-Loaded Polyfluorene Light-Harvesting Polymer, J. Phys. Chem. Lett. 3 (2012) 2453–2457, https://doi.org/10.1021/jz300979j.
[46] M. Natali, M. Ravaglia, F. Scandola, J. Boixel, Y. Pellegrin, E. Blart, F. Odobel, Long-Range Charge Separation in a Ferrocene–(Zinc Porphyrin)–Naphthalenediimide Triad. Asymmetric Role of 1,2,3-Triazole Linkers, J. Phys. Chem. C. 117 (2013) 19334–19345, https://doi.org/10.1021/jp406405k.
[47] E.A. Ermilov, M. Schlak, R. Steffen, X.Q. Liu, J.Y. Liu, B. Röder, Energy transfer properties of a novel boron dipyrromethene-perylenediimide donor-acceptor dyad, RSC Adv. 5 (2015) 67141–67148, https://doi.org/10.1039/c5ra10077a.
[48] G. de Miguel, M. Wielopolski, D.I. Schuster, M.A. Fazio, O.P. Lee, C.K. Haley, A. L. Ortiz, L. Echegoyen, T. Clark, D.M. Guldi, Triazole Bridges as Versatile Linkers in Electron Donor-Acceptor Conjugates, J. Am. Chem. Soc. 133 (2011) 13036–13054, https://doi.org/10.1021/ja202485s.
[49] J. Mohanraj, A. Barbieri, N. Armaroli, M. Vizuete, F. Langa, B. Delavaux-Nicot, M. Vartanian, J. Iehl, U. Hahn, J.-F. Nierengarten, Efficient Photoinduced Energy and Electron Transfer in Zn II -Porphyrin/Fullerene Dyads with Interchromophoric Distances up to 2.6 nm and No Wire-like Connectivity, Chem. – A Eur. J. 23 (2017) 14200–14212, https://doi.org/10.1002/chem.201701668.
[50] C. Villegas, J.L. Delgado, P.-A. Bouit, B. Grimm, W. Seitz, N. Martín, D.M. Guldi, Powering reductive charge shift reactions—linking fullerenes of different

electron acceptor strength to secure an energy gradient, Chem. Sci. 2 (2011) 1677, https://doi.org/10.1039/c1sc00331c.
[51] K.-H. Le Ho, I. Hijazi, L. Rivier, C. Gautier, B. Jousselme, G. de Miguel, C. Romero-Nieto, D.M. Guldi, B. Heinrich, B. Donnio, S. Campidelli, Host-Guest Complexation of [60]Fullerenes and Porphyrins Enabled by "Click Chemistry", Chem. – A Eur. J. 19 (2013) 11374–11381, https://doi.org/10.1002/chem.201300793.
[52] G. Leem, Z.A. Morseth, E. Puodziukynaite, J. Jiang, Z. Fang, A.T. Gilligan, J.R. Reynolds, J.M. Papanikolas, K.S. Schanze, Light Harvesting and Charge Separation in a π-Conjugated Antenna Polymer Bound to TiO 2, J. Phys. Chem. C. 118 (2014) 28535–28541, https://doi.org/10.1021/jp5113558.
[53] S. Pla, L. Martín-Gomis, K. Ohkubo, S. Fukuzumi, F. Fernández-Lázaro, Á. Sastre-Santos, Macrocyclic Dyads Based on C 60 and Perylenediimides Connected by Click Chemistry, Asian, J. Org. Chem. 3 (2014) 185–197, https://doi.org/10.1002/ajoc.201300235.
[54] A. Labrunie, J. Gorenflot, M. Babics, O. Alévêque, S. Dabos-Seignon, A.H. Balawi, Z. Kan, M. Wohlfahrt, E. Levillain, P. Hudhomme, P.M. Beaujuge, F. Laquai, C. Cabanetos, P. Blanchard, Triphenylamine-Based Push-Pull σ–C 60 Dyad As Photoactive Molecular Material for Single-Component Organic Solar Cells: Synthesis, Characterizations, and Photophysical Properties, Chem. Mater. 30 (2018) 3474–3485, https://doi.org/10.1021/acs.chemmater.8b01117.
[55] F. Zieschang, M.H. Schreck, A. Schmiedel, M. Holzapfel, J.H. Klein, C. Walter, B. Engels, C. Lambert, Photoinduced Electron Transfer Dynamics in Triarylamine-Naphthalene Diimide Cascades, J. Phys. Chem. C. 118 (2014) 27698–27714, https://doi.org/10.1021/jp5085058.
[56] N.T. Nguyen, J. Hofkens, I.G. Scheblykin, M. Kruk, W. Dehaen, Click Reaction Synthesis and Photophysical Studies of Dendritic Metalloporphyrins, European J. Org. Chem. 2014 (2014) 1766–1777, https://doi.org/10.1002/ejoc.201301158.
[57] Y. Pareek, M. Ravikanth, Synthesis and properties of porphyrin-expanded porphyrin click dyads, Tetrahedron. 69 (2013) 7943–7949, https://doi.org/10.1016/j.tet.2013.07.013.
[58] B. Brizet, N. Desbois, A. Bonnot, A. Langlois, A. Dubois, J.-M. Barbe, C.P. Gros, C. Goze, F. Denat, P.D. Harvey, Slow and Fast Singlet Energy Transfers in BODIPY-gallium(III)corrole Dyads Linked by Flexible Chains, Inorg. Chem. 53 (2014) 3392–3403, https://doi.org/10.1021/ic402798f.
[59] K. Yoosaf, J. Iehl, I. Nierengarten, M. Hmadeh, A.-M. Albrecht-Gary, J.-F. Nierengarten, N. Armaroli, A Supramolecular Photosynthetic Model Made of a Multiporphyrinic Array Constructed around a C 60 Core and a C 60 -Imidazole Derivative, Chem. – A Eur. J. 20 (2014) 223–231, https://doi.org/10.1002/chem.201303481.
[60] M.A. Fazio, O.P. Lee, D.I. Schuster, First triazole-linked porphyrin-fullerene dyads, Org. Lett. 10 (2008) 4979–4982, https://doi.org/10.1021/ol802053k.
[61] D.K. Singh, M. Nath, Meso-Phenyl-triazole bridged porphyrin-coumarin dyads: Synthesis, characterization and photophysical properties, Dye. Pigment. 121 (2015) 256–264, https://doi.org/10.1016/j.dyepig.2015.05.027.
[62] V.S. Shetti, M. Ravikanth, Synthesis of Triazole-Bridged Unsymmetrical Porphyrin Dyads and Porphyrin-Ferrocene Conjugates, European J. Org. Chem. 2010 (2010) 494–508, https://doi.org/10.1002/ejoc.200901070.
[63] O. Rezazgui, P. Trouillas, S. Qiu, B. Siegler, J. Gierschner, S. Leroy-Lhez, Synthesis and conformation of a novel fluorescein–Zn-porphyrin dyad and intramolecular energy transfer, New J. Chem. 40 (2016) 3843–3856, https://doi.org/10.1039/C5NJ02901E.
[64] A. Charisiadis, E. Giannoudis, Z. Pournara, A. Kosma, V. Nikolaou, G. Charalambidis, V. Artero, M. Chavarot-Kerlidou, A.G. Coutsolelos, Synthesis and Characterization of a Covalent Porphyrin-Cobalt Diimine-Dioxime Dyad for Photoelectrochemical H2 Evolution, Eur. J. Inorg. Chem. 2021 (2021) 1122–1129, https://doi.org/10.1002/ejic.202001111.
[65] F. Brégier, S.M. Aly, C.P. Gros, J.-M. Barbe, Y. Rousselin, P.D. Harvey, Design and Photophysical Properties of Zinc(II) Porphyrin-Containing Dendrons Linked to a Central Artificial Special Pair, Chem. – A Eur. J. 17 (2011) 14643–14662, https://doi.org/10.1002/chem.201101832.
[66] S. Punidha, J. Sinha, A. Kumar, M. Ravikanth, First Triazole-Bridged Unsymmetrical Porphyrin Dyad via Click Chemistry, J. Org. Chem. 73 (2008) 323–326, https://doi.org/10.1021/jo702018s.
[67] P. Farràs, A.C. Benniston, Bodipy-ruthenium(II) tris-bipyridyl dyads for homogeneous photochemical oxidations, Tetrahedron Lett. 55 (2014) 7011–7014, https://doi.org/10.1016/j.tetlet.2014.10.119.
[68] M. Ramachandran, S. Anandan, M. Ashokkumar, A luminescent on–off probe based calix[4]arene linked through triazole with ruthenium(<scp>ii</scp>) polypyridine complexes to sense copper(<scp>ii</scp>) and sulfide ions, New J. Chem. 43 (2019) 9832–9842, https://doi.org/10.1039/C9NJ01632E.
[69] J.-Y. Liu, M.E. El-Khouly, S. Fukuzumi, D.K.P. Ng, Mimicking Photosynthetic Antenna-Reaction-Center Complexes with a (Boron Dipyrromethene)3-Porphyrin-C60 Pentad, Chem. – A Eur. J. 17 (2011) 1605–1613, https://doi.org/10.1002/chem.201002333.
[70] J. Iehl, I. Osinska, R. Louis, M. Holler, J.-F.-F. Nierengarten, A stable fullerene-azide building block for the construction of a fullerene-porphyrin conjugate, Tetrahedron Lett. 50 (2009) 2245–2248, https://doi.org/10.1016/j.tetlet.2009.02.185.
[71] S. Sheth, A. Baron, C. Herrero, B. Vauzeilles, A. Aukauloo, W. Leibl, Light-induced tryptophan radical generation in a click modular assembly of a sensitiser-tryptophan residue, Photochem. Photobiol. Sci. 12 (2013) 1074, https://doi.org/10.1039/c3 pp50021g.
[72] A. Baron, C. Herrero, A. Quaranta, M.-F. Charlot, W. Leibl, B. Vauzeilles, A. Aukauloo, Click Chemistry on a Ruthenium Polypyridine Complex. An Efficient and Versatile Synthetic Route for the Synthesis of Photoactive Modular Assemblies, Inorg. Chem. 51 (2012) 5985–5987, https://doi.org/10.1021/ic300227j.
[73] J. Iehl, M. Vartanian, M. Holler, J.-F. Nierengarten, B. Delavaux-Nicot, J.-M. Strub, A. Van Dorsselaer, Y. Wu, J. Mohanraj, K. Yoosaf, N. Armaroli, Photoinduced electron transfer in a clicked fullerene–porphyrin conjugate, J. Mater. Chem. 21 (2011) 1562–1573, https://doi.org/10.1039/C0JM02310H.
[74] A. Eggenspiller, A. Takai, M.E. El-Khouly, K. Ohkubo, C.P. Gros, C. Bernhard, C. Goze, F. Denat, J. Barbe, S. Fukuzumi, Synthesis and Photodynamics of Fluorescent Blue BODIPY-Porphyrin Tweezers Linked by Triazole Rings, J. Phys. Chem. A. 116 (2012) 3889–3898, https://doi.org/10.1021/jp300415a.
[75] A. Harriman, K.J. Elliott, M.A.H. Alamiry, L. Le Pleux, M. Séverac, Y. Pellegrin, E. Blart, C. Fosse, C. Cannizzo, C.R. Mayer, F. Odobel, Intramolecular Electron Transfer Reactions Observed for Dawson-Type Polyoxometalates Covalently Linked to Porphyrin Residues, J. Phys. Chem. C. 113 (2009) 5834–5842, https://doi.org/10.1021/jp900643m.
[76] P. Gotico, T.T. Tran, A. Baron, B. Vauzeilles, C. Lefumeux, M.H. Ha-Thi, T. Pino, Z. Halime, A. Quaranta, W. Leibl, A. Aukauloo, Tracking Charge Accumulation in a Functional Triazole-Linked Ruthenium-Rhenium Dyad Towards Photocatalytic Carbon Dioxide Reduction, ChemPhotoChem. 5 (2021) 654–664, https://doi.org/10.1002/cptc.202100010.
[77] S. Cetindere, S.T. Clausing, M. Anjass, Y. Luo, S. Kupfer, B. Dietzek, C. Streb, Covalent Linkage of BODIPY-Photosensitizers to Anderson-Type Polyoxometalates Using CLICK Chemistry, Chem. – A Eur. J. 27 (2021) 17181–17187, https://doi.org/10.1002/chem.202102897.
[78] K.J. Elliott, A. Harriman, L. Le Pleux, Y. Pellegrin, E. Blart, C.R. Mayer, F. Odobel, A porphyrin–polyoxometallate bio-inspired mimic for artificial photosynthesis, Phys. Chem. Chem. Phys. 11 (2009) 8767, https://doi.org/10.1039/b905548g.
[79] M. Fathalla, J.C. Barnes, R.M. Young, K.J. Hartlieb, S.M. Dyar, S.W. Eaton, A.A. Sarjeant, D.T. Co, M.R. Wasielewski, J.F. Stoddart, Photoinduced Electron Transfer within a Zinc Porphyrin-Cyclobis(paraquat- p -phenylene) Donor-Acceptor Dyad, Chem. – A Eur. J. 20 (2014) 14690–14697, https://doi.org/10.1002/chem.201403744.
[80] L. Le Pleux, Y. Pellegrin, E. Blart, F. Odobel, A. Harriman, Long-Lived, Charge-Shift States in Heterometallic, Porphyrin-Based Dendrimers Formed via Click Chemistry, J. Phys. Chem. A. 115 (2011) 5069–5080, https://doi.org/10.1021/jp2012182.
[81] V. Nikolaou, K. Karikis, Y. Farré, G. Charalambidis, F. Odobel, A.G. Coutsolelos, Click made porphyrin–corrole dyad: a system for photo-induced charge separation, Dalt. Trans. 44 (2015) 13473–13479, https://doi.org/10.1039/C5DT01730K.
[82] E. Ganapathi, S. Madhu, M. Ravikanth, Synthesis and properties of triazole bridged BODIPY-conjugates, Tetrahedron. 70 (2014) 664–671, https://doi.org/10.1016/j.tet.2013.11.091.
[83] P.B. Pati, L. Zhang, B. Philippe, R. Fernández-Terán, S. Ahmadi, L. Tian, H. Rensmo, L. Hammarström, H. Tian, Insights into the Mechanism of a Covalently Linked Organic Dye-Cobaloxime Catalyst System for Dye-Sensitized Solar Fuel Devices, ChemSusChem. 10 (2017) 2480–2495, https://doi.org/10.1002/cssc.201700285.
[84] S. Bold, J. Massin, E. Giannoudis, M. Koepf, V. Artero, B. Dietzek, M. Chavarot-Kerlidou, Spectroscopic Investigations Provide a Rationale for the Hydrogen-Evolving Activity of Dye-Sensitized Photocathodes Based on a Cobalt Tetraazamacrocyclic Catalyst, ACS Catal. 11 (2021) 3662–3678, https://doi.org/10.1021/acscatal.0c05033.
[85] E. Giannoudis, S. Bold, C. Müller, A. Schwab, J. Bruhnke, N. Queyriaux, C. Gablin, D. Leonard, C. Saint-Pierre, D. Gasparutto, D. Aldakov, S. Kupfer, V. Artero, B. Dietzek, M. Chavarot-Kerlidou, Hydrogen Production at a NiO Photocathode Based on a Ruthenium Dye-Cobalt Diimine Dioxime Catalyst Assembly: Insights from Advanced Spectroscopy and Post-operando Characterization, ACS Appl. Mater. Interfaces. 13 (2021) 49802–49815, https://doi.org/10.1021/acsami.1c12138.
[86] N. Queyriaux, E.S. Andreiadis, S. Torelli, J. Pecaut, B.S. Veldkamp, E.A. Margulies, M.R. Wasielewski, M. Chavarot-Kerlidou, V. Artero, CuAAC-based assembly and characterization of a ruthenium–copper dyad containing a diimine–dioxime ligand framework, Faraday Discuss. 198 (2017) 251–261, https://doi.org/10.1039/C6FD00204H.
[87] C. Herrero, A. Quaranta, S. El Ghachtouli, B. Vauzeilles, W. Leibl, A. Aukauloo, Carbon dioxide reduction via light activation of a ruthenium–Ni(cyclam) complex, Phys. Chem. Chem. Phys. 16 (2014) 12067, https://doi.org/10.1039/c3cp54946a.
[88] C. Herrero, A. Quaranta, M. Sircoglou, K. Sénéchal-David, A. Baron, I.M. Marín, C. Buron, J.-P. Baltaze, W. Leibl, A. Aukauloo, F. Banse, Successive light-induced two electron transfers in a Ru–Fe supramolecular assembly: from Ru–Fe(<scp>ii</scp>)–OH $_2$ to Ru–Fe(<scp>iv</scp>)–oxo, Chem. Sci. 6 (2015) 2323–2327, https://doi.org/10.1039/C5SC00024F.
[89] A.G. Tebo, A. Quaranta, C. Herrero, V.L. Pecoraro, A. Aukauloo, Intramolecular Photogeneration of a Tyrosine Radical in a Designed Protein, ChemPhotoChem. 1 (2017) 89–92, https://doi.org/10.1002/cptc.201600044.
[90] T. Schlotthauer, R. Schroot, S. Glover, L. Hammarström, M. Jäger, U.S. Schubert, A multidonor–photosensitizer–multiacceptor triad for long-lived directional charge separation, Phys. Chem. Chem. Phys. 19 (2017) 28572–28578, https://doi.org/10.1039/C7CP05593E.

[91] A. Nantalaksakul, A. Mueller, A. Klaikherd, C.J. Bardeen, S. Thayumanavan, Dendritic and Linear Macromolecular Architectures for Photovoltaics: A Photoinduced Charge Transfer Investigation, J. Am. Chem. Soc. 131 (2009) 2727–2738, https://doi.org/10.1021/ja809194u.
[92] A. Baron, C. Herrero, A. Quaranta, M.-F. Charlot, W. Leibl, B. Vauzeilles, A. Aukauloo, Efficient electron transfer through a triazole link in ruthenium(ii) polypyridine type complexes, Chem. Commun. 47 (2011) 11011, https://doi.org/10.1039/c1cc13683f.
[93] F. Odobel, M. Séverac, Y. Pellegrin, E. Blart, C. Fosse, C. Cannizzo, C.R. Mayer, K. J. Elliott, A. Harriman, Coupled Sensitizer-Catalyst Dyads: Electron-Transfer Reactions in a Perylene-Polyoxometalate Conjugate, Chem. – A Eur. J. 15 (2009) 3130–3138, https://doi.org/10.1002/chem.200801880.
[94] C. Herrero, L. Batchelor, A. Baron, S. El Ghachtouli, S. Sheth, R. Guillot, B. Vauzeilles, M. Sircoglou, T. Mallah, W. Leibl, A. Aukauloo, Click Chemistry as a Convenient Tool for the Incorporation of a Ruthenium Chromophore and a Nickel-Salen Monomer into a Visible-Light-Active Assembly, Eur. J. Inorg. Chem. 2013 (2013) 494–499, https://doi.org/10.1002/ejic.201201161.
[95] M. Natali, S. Campagna, F. Scandola, Photoinduced electron transfer across molecular bridges: electron- and hole-transfer superexchange pathways, Chem. Soc. Rev. 43 (2014) 4005–4018, https://doi.org/10.1039/C3CS60463B.
[96] B. Mayoh, P. Day, Charge transfer in mixed valence solids. Part VII. Perturbation calculations of valence delocalization in iron(II, III) cyanides and silicates, J. Chem. Soc. Dalt. Trans. (1974) 846, https://doi.org/10.1039/dt9740000846.
[97] H.M. McConnell, Intramolecular Charge Transfer in Aromatic Free Radicals, J. Chem. Phys. 35 (1961) 508–515, https://doi.org/10.1063/1.1731961.
[98] J. Halpern, L.E. Orgel, The theory of electron transfer between metal ions in bridged systems, Discuss. Faraday Soc. 29 (1960) 32, https://doi.org/10.1039/df9602900032.
[99] V. Novakova, P. Hladík, T. Filandrová, I. Zajícová, V. Krepsová, M. Miletin, J. Lenčo, P. Zimcik, Structural factors influencing the intramolecular charge transfer and photoinduced electron transfer in tetrapyrazinoporphyrazines, Phys. Chem. Chem. Phys. 16 (2014) 5440–5446, https://doi.org/10.1039/c3cp54731k.
[100] T. Higashino, T. Yamada, M. Yamamoto, A. Furube, N.V. Tkachenko, T. Miura, Y. Kobori, R. Jono, K. Yamashita, H. Imahori, Remarkable Dependence of the Final Charge Separation Efficiency on the Donor-Acceptor Interaction in Photoinduced Electron Transfer, Angew. Chemie – Int. Ed. 55 (2016) 629–633, https://doi.org/10.1002/anie.201509067.
[101] J.R. Cann, C. Cabanetos, G.C. Welch, Synthesis of Molecular Dyads and Triads Based Upon N-Annulated Perylene Diimide Monomers and Dimers, European J. Org. Chem. 2018 (2018) 6933–6943, https://doi.org/10.1002/ejoc.201801383.
[102] R.A. Marcus, N. Sutin, Electron transfers in chemistry and biology, Biochim. Biophys. Acta – Rev. Bioenerg. 811 (1985) 265–322, https://doi.org/10.1016/0304-4173(85)90014-X.
[103] O.S. Wenger, How Donor – Bridge – Acceptor energetics influence electron tunneling dynamics and their distance dependences, Acc. Chem. Res. 44 (2011) 25–35, https://doi.org/10.1021/ar100092v.
[104] M. Gilbert, B. Albinsson, Photoinduced charge and energy transfer in molecular wires, Chem. Soc. Rev. 44 (2015) 845–862, https://doi.org/10.1039/c4cs00221k.
[105] U. Hahn, J.F. Nierengarten, The copper-catalyzed alkyne-azide cycloaddition for the construction of fullerene-porphyrin conjugates, J. Porphyr. Phthalocyanines. 20 (2016) 918–934, https://doi.org/10.1142/S1088424616500966.
[106] S.V. Kirner, D.M. Guldi, J.D. Megiatto, D.I. Schuster, Synthesis and photophysical properties of new catenated electron donor-acceptor materials with magnesium and free base porphyrins as donors and C60 as the acceptor, Nanoscale. 7 (2015) 1145–1160, https://doi.org/10.1039/c4nr06146b.
[107] M. Braumüller, M. Staniszewska, J. Guthmuller, S. Rau, CLICK "n" Sleep: Light-Switch Behavior of Triazole-Containing Tris(bipyridyl)ruthenium Complexes, Eur. J. Inorg. Chem. 2016 (2016) 4958–4963, https://doi.org/10.1002/ejic.201600964.
[108] J.D. Megiatto, D.I. Schuster, S. Abwandner, G. de Miguel, D.M. Guldi, [2] Catenanes Decorated with Porphyrin and [60]Fullerene Groups: Design, Convergent Synthesis, and Photoinduced Processes, J. Am. Chem. Soc. 132 (2010) 3847–3861, https://doi.org/10.1021/ja910149f.
[109] C. Lee, W. Yang, R.G. Parr, Development of the Colle-Salvetti correlation-energy formula into a functional of the electron density, Phys. Rev. B. 37 (1988) 785–789, https://doi.org/10.1103/PhysRevB.37.785.
[110] A. Becke, Density-functional thermochemistry. III. The role of exact exchange, J. Chem. Phys. 98 (1993) 5648–5652, https://doi.org/10.1063/1.464913.
[111] F. Weigend, R. Ahlrichs, Balanced basis sets of split valence, triple zeta valence and quadruple zeta valence quality for H to Rn: Design and assessment of accuracy, Phys. Chem. Chem. Phys. 7 (2005) 3297, https://doi.org/10.1039/b508541a.
[112] P.J. Hay, W.R. Wadt, Ab initio effective core potentials for molecular calculations. Potentials for the transition metal atoms Sc to Hg, J. Chem. Phys. 82 (1985) 270–283, https://doi.org/10.1063/1.448799.
[113] A. Kroll, K. Monczak, D. Sorsche, S. Rau, A Luminescent Ruthenium Azide Complex as a Substrate for Copper-Catalyzed Click Reactions, Eur. J. Inorg. Chem. 2014 (2014) 3462–3466, https://doi.org/10.1002/ejic.201402395.
[114] K.P. Chitre, E. Guillén, A.S. Yoon, E. Galoppini, Synthesis of Homoleptic Ruthenium "Star" Complexes by Click Reaction for TiO 2 Sensitization, Eur. J. Inorg. Chem. 2012 (2012) 5461–5464, https://doi.org/10.1002/ejic.201200896.
[115] T.H. Dunning, Gaussian basis sets for use in correlated molecular calculations. I. The atoms boron through neon and hydrogen, J. Chem. Phys. 90 (2) (1989) 1007–1023.
[116] T. Yanai, D.P. Tew, N.C. Handy, A new hybrid exchange–correlation functional using the Coulomb-attenuating method (CAM-B3LYP), Chem. Phys. Lett. 393 (2004) 51–57, https://doi.org/10.1016/j.cplett.2004.06.011.